CSTS

Consortium to Study Trends in Seismicity

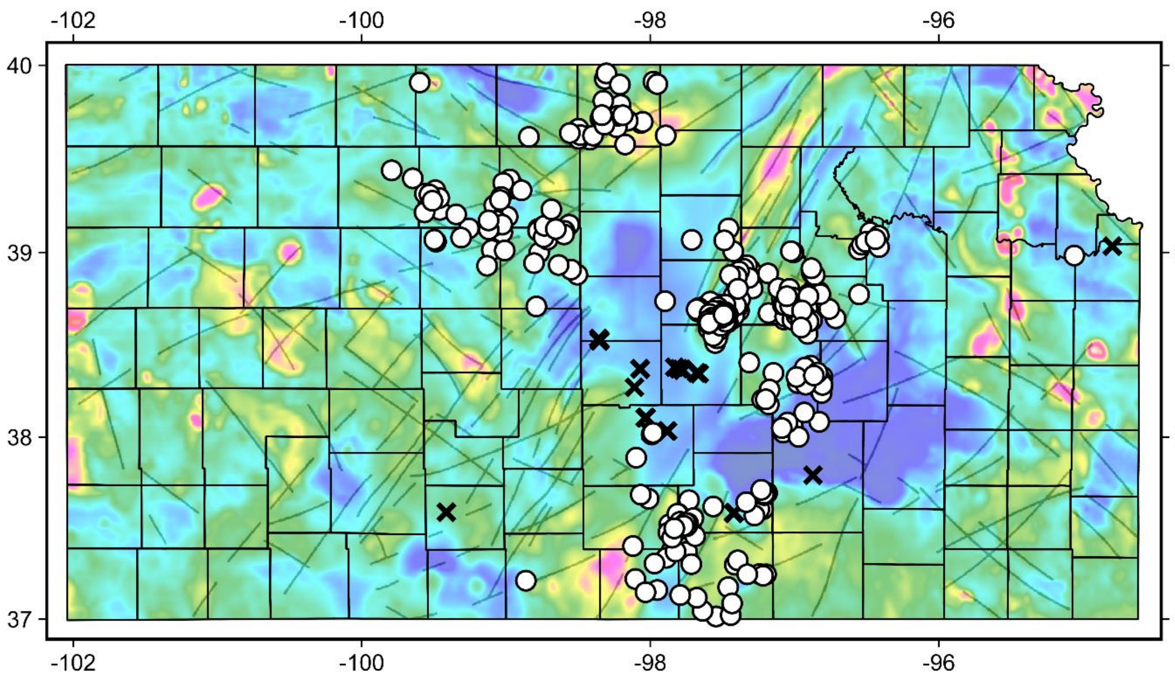

July 1, 2021 – June 30, 2022

Annual Report by
Rex Buchanan, Shelby Peterie, and Rick Miller

Kansas Geological Survey Open-file Report 2023-51

Cover Figure Caption: Earthquakes (white) located using CSTS stations that otherwise would not have been located by any other seismic network overlaying the state aeromagnetic map in color. Correlated with structural trends, the earthquakes provide insight into the stress conditions and relative stability of both unmapped faults and faults interpreted from geologic and geophysical datasets.

Kansas Geological Survey
Consortium to Study Trends in Seismicity

2021-2022 Annual Report

NOTICE: This annual report was released in draft form to Consortium members, as well as the Kansas Department of Health and Environment, on August 30, 2022, and was subject to further review and comment by Consortium members until November 30, 2022. The KGS was then allowed an additional three months to revise the draft report and distribute the final annual report.

CONSORTIUM TO STUDY TRENDS IN SEISMICITY
KANSAS GEOLOGICAL SURVEY
Fourth Quarter / Annual Report
July 1, 2021 – June 30, 2022

INTRODUCTION

The Kansas Geological Survey's Consortium to Study Trends in Seismicity (CSTS) is a public-private project aimed at studying trends in seismicity in Kansas. The consortium focuses on areas where public and private entities could benefit from high-sensitivity seismic monitoring and scientifically supported projections. Seismicity has increased significantly in Kansas and the midcontinent since 2013, leading to a need to better define and understand earthquake activity, particularly as it relates to subsurface fluid disposal. The CSTS oversees the operation of a seismic network that records and allows accurate location and magnitude estimates of seismicity for felt earthquakes and particularly for microseismic events that are hundreds of times smaller than can be routinely identified with previous regional seismic networks. Understanding current micro-trends in seismicity and establishing a data-driven awareness of potential factors affecting seismicity should help with industry response, guide governmental oversight, and inform public opinion.

The CSTS is operated by the Kansas Geological Survey (KGS), a research and service division of the University of Kansas with a long history of studying the state's subsurface and seismic issues. Current members of the CSTS are from the state's Class I disposal well community (Class I wells are used for disposal of municipal and industrial waste and regulated by the Kansas Department of Health and Environment [KDHE]). Membership in the CSTS is voluntary and open to any industry partner; the CSTS objective is identifying and understanding seismicity at magnitudes down to zero in proximity to member facilities. The CSTS works to establish baseline or background seismicity near those facilities, provide a scientific basis for differentiating natural from induced seismicity, and predict future earthquake occurrences. Confidence in distinguishing natural from induced earthquake trends and predicting future occurrences is greatly enhanced through extended monitoring periods relying on stations near earthquake epicenters.

The following report describes the fifth year of CSTS activities, including a discussion of membership status; network station installation and operation; earthquakes recorded and identified, and earthquake alerts provided to members; web page development; other activities, especially involving publications, presentations, and meeting attendance; and plans for the coming year. Three quarterly reports were provided to members since the Consortium's annual meeting in August 2021. This current report includes summaries of seismicity and CSTS activities in the past quarter (April, May, and June of 2022) as well as the past 12 months.

STATUS OF MEMBERS

The CSTS was established with a two-tier membership system. For Tier 1 members the CSTS provides equipment, installation, and monitoring of a seismograph station; maintains a catalog of seismic events, updated weekly, with a goal of providing e-mail alerts within 24 hours or less of any earthquakes greater than magnitude 2 within 30 miles of a facility; provides quarterly reports of monitoring findings; and hosts an annual meeting at which results are discussed and plans formulated for the coming year. Tier 2 members have access to information related to the general seismicity being studied by the CSTS and can attend the annual meeting, but do not have the right to vote at that meeting or use the reports while still under confidential status. The CSTS currently has eleven Tier 1 members.

STATUS OF NETWORK

The CSTS seismic network currently consists of twelve stations in Ellsworth, Rice, McPherson, Reno, Kiowa, Sedgwick, Butler, Johnson, and Atchison counties, Kansas (Figure 1, Appendix A). Waveforms for these stations are available for Tier 1 members on the seismic network page of the CSTS website. For each of those locations, ambient noise tests were completed to establish background noise levels. Those tests identified noise from nearby highways, trains, pump jacks, and other facilities that might interfere with earthquake analysis. Stations were relocated when initially deployed in places where noise and vibrations interfered with station response characteristics above a pre-determined threshold as determined by a site-specific ambient noise test. Many of the existing sites are in cemeteries, on government property, or in locations where noise levels are measured and determined to be low and likely to remain low. In all cases, KGS has obtained written agreements with landowners of each station location.

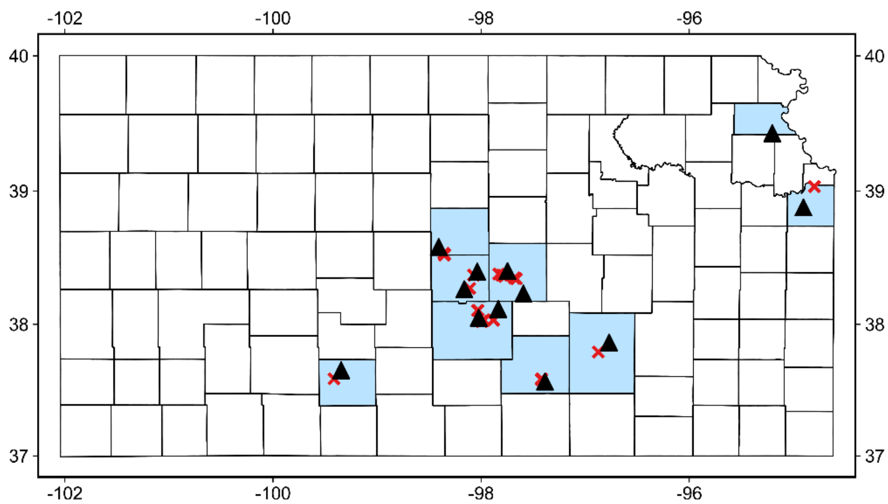

Figure 1. Earthquake stations (black triangles) with member facilities (red X) provide high sensitivity coverage with the potential to identify earthquakes with magnitudes below 0 within 20 miles of each facility.

Each station consists of a seismic sensor that includes a shallowly buried seismometer embedded in a concrete platform atop a gravel layer and a digitizer (Figure 2). Ground motion detected by the seismometer is transmitted back to KGS offices in Lawrence real-time via a cellular modem. That communication system is powered by a solar panel that charges two deep-cycle marine batteries. The footprint for each station is approximately 10 feet by 10 feet. The

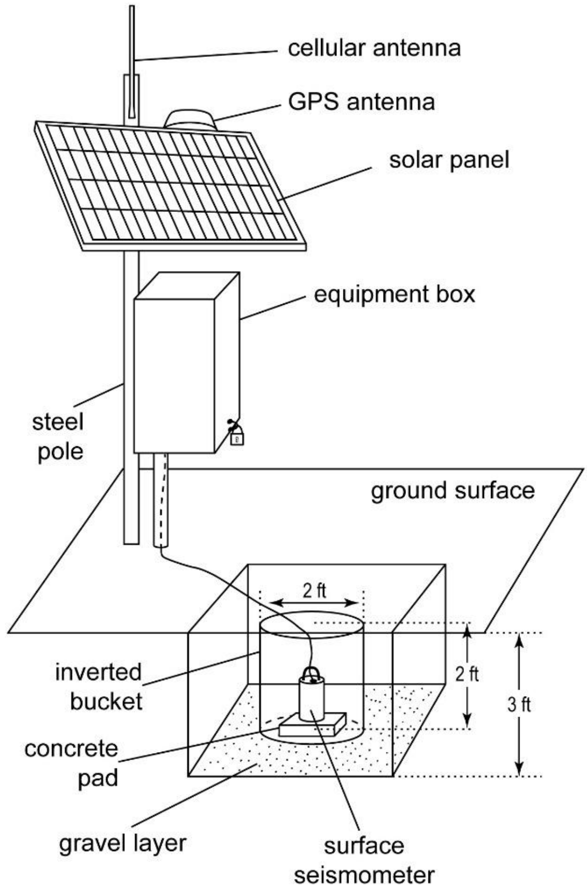

Figure 2. Diagram illustrating a temporary seismic installation.

stations operated over the last year with a better than 98% continuous data stream and within designated operational sensitivity and signal-to-noise ratio.

EARTHQUAKE ALERTS, CATALOG

Earthquakes with magnitudes of 2 or larger represent a threshold above which energy levels provide highly confident automatic analysis for feeds coming from a network as dense as the CSTS network and especially in conjunction with the KGS regional and subregional networks. It is therefore reasonable to provide accurate epicenter locations using automated picking routines for each event down to M 2, with results available within minutes of the fault rupture and release of energy. KGS staff notify CSTS members of a magnitude (M) 2 or larger earthquake within 30 miles of Tier 1 member wells. Earthquakes below magnitude 2.5 are generally considered below felt levels. Earthquakes with magnitudes down to 1 can be located with confidence in areas where at least three CSTS stations are within 50 miles of each other. There were 248 earthquake alerts from July 2021 through June 2022 (Table 1), more than double the alerts in the 2020-2021 reporting year. More than 200 of the alerts were for events in Saline County, where seismicity dramatically increased, as discussed in later sections.

Table 1. M 2 or larger earthquakes recorded from July 2021 through June 2022 with epicenters located within 30 mi of member wells.

Origin Time (UTC)	Latitude	Longitude	Magnitude	County
2021-07-03 01:30:16	37.50163	-97.77737	2.0	Sedgwick
2021-07-05 12:06:19	37.69272	-97.24539	2.1	Sedgwick
2021-07-05 13:31:59	37.69020	-97.21140	2.0	Sedgwick
2021-07-17 02:43:10	38.01585	-97.98830	2.6	Reno
2021-07-17 03:06:06	38.01985	-97.99049	2.4	Reno
2021-07-17 08:12:19	38.01519	-97.99129	2.7	Reno
2021-07-26 15:26:45	38.64783	-97.43725	2.4	Saline
2021-08-05 18:28:13	37.65158	-97.56013	2.1	Sedgwick
2021-08-14 16:15:30	38.65718	-97.45670	2.0	Saline
2021-08-16 20:50:20	38.64991	-97.45454	2.1	Saline
2021-08-21 10:54:33	38.64590	-97.44786	1.8	Saline
2021-09-02 15:36:48	38.70734	-97.60008	2.0	Saline
2021-09-28 09:14:37	38.64973	-97.45556	2.5	Saline
2021-09-28 09:26:19	38.64759	-97.43401	2.1	Saline
2021-09-29 03:46:57	38.67295	-97.49376	2.1	Saline
2021-10-03 23:02:40	38.68123	-97.59728	2.6	Saline
2021-10-04 02:58:13	38.65478	-97.46830	3.8	Saline
2021-10-04 08:54:28	38.68498	-97.62930	2.5	Saline
2021-10-04 17:12:08	38.67990	-97.63168	2.2	Saline
2021-10-04 22:01:52	38.67979	-97.61574	2.1	Saline
2021-10-06 09:00:37	38.65909	-97.45767	1.9	Saline
2021-10-07 14:25:12	38.64698	-97.46420	2.0	Saline
2021-10-12 12:48:27	38.68164	-97.63229	2.1	Saline
2021-10-17 16:45:23	38.07130	-96.79294	2.3	Butler
2021-10-22 08:57:44	37.50817	-97.79712	2.2	Sedgwick
2021-10-24 22:33:11	37.63918	-97.26352	2.5	Sedgwick
2021-11-01 18:43:35	38.67888	-97.60531	2.2	Saline
2021-11-03 21:12:34	38.67926	-97.46307	3.1	Saline
2021-11-05 10:47:38	38.65623	-97.46278	2.4	Saline
2021-11-06 04:59:38	38.66225	-97.44618	2.1	Saline
2021-11-08 06:20:56	38.66697	-97.45671	2.8	Saline
2021-11-08 06:46:26	38.65715	-97.47018	2.6	Saline
2021-11-09 12:19:05	38.67320	-97.46131	3.2	Saline
2021-11-13 17:17:36	38.66256	-97.44981	2.1	Saline
2021-11-14 17:45:47	38.65415	-97.46627	2.4	Saline
2021-11-14 17:53:56	38.65691	-97.45110	2.1	Saline
2021-11-15 02:18:27	38.66111	-97.49777	1.9	Saline
2021-11-16 06:37:06	38.70186	-97.43253	2.2	Saline
2021-11-17 21:43:09	38.66584	-97.44717	3.2	Saline
2021-11-18 01:40:04	38.65409	-97.44295	2.9	Saline
2021-11-18 14:20:29	38.67073	-97.51909	3.2	Saline
2021-11-18 21:43:53	38.65005	-97.44902	2.2	Saline
2021-11-19 08:57:54	38.66556	-97.45581	1.8	Saline
2021-11-20 12:22:29	38.24260	-97.48433	2.2	McPherson
2021-12-04 01:28:21	38.69096	-97.54217	2.2	Saline
2021-12-04 06:59:44	38.69036	-97.59721	2.2	Saline
2021-12-04 10:32:25	38.68871	-97.59777	2.4	Saline
2021-12-04 17:31:33	38.68805	-97.58183	2.1	Saline
2021-12-08 13:45:27	38.66091	-97.46556	4.6	Saline
2021-12-08 13:59:00	38.66066	-97.48277	2.7	Saline
2021-12-08 14:11:48	38.64829	-97.46660	2.3	Saline
2021-12-08 14:21:47	38.66167	-97.47086	2.7	Saline
2021-12-08 15:02:38	38.66229	-97.46520	2.0	Saline
2021-12-08 15:12:31	38.66138	-97.49241	2.4	Saline
2021-12-08 15:14:57	38.65981	-97.46523	2.4	Saline
2021-12-08 15:25:54	38.65840	-97.46986	2.8	Saline
2021-12-08 15:44:24	38.66431	-97.47925	2.1	Saline
2021-12-08 16:48:15	38.65929	-97.49020	2.0	Saline
2021-12-08 19:55:57	38.64919	-97.46382	2.0	Saline

Table 1. Continued

Origin Time (UTC)	Latitude	Longitude	Magnitude	County
2021-12-08 19:59:06	38.64802	-97.46843	2.1	Saline
2021-12-08 20:25:42	38.65403	-97.46187	3.2	Saline
2021-12-09 01:12:29	38.65583	-97.45474	2.3	Saline
2021-12-09 03:07:10	38.67174	-97.44330	2.2	Saline
2021-12-09 06:14:23	38.65494	-97.45934	1.8	Saline
2021-12-09 20:26:00	38.67556	-97.45431	2.4	Saline
2021-12-09 20:57:10	38.65758	-97.48093	2.0	Saline
2021-12-10 00:54:00	38.66970	-97.46980	1.9	Saline
2021-12-10 01:59:04	38.64612	-97.44437	2.6	Saline
2021-12-10 02:11:20	38.66551	-97.48697	1.9	Saline
2021-12-10 18:12:52	38.66430	-97.46504	1.9	Saline
2021-12-11 03:56:00	38.64738	-97.43844	2.2	Saline
2021-12-11 10:28:19	38.65263	-97.46765	2.4	Saline
2021-12-11 11:18:30	38.64944	-97.45801	2.3	Saline
2021-12-11 11:41:52	38.65543	-97.46479	1.8	Saline
2021-12-11 12:40:34	38.66369	-97.46551	2.1	Saline
2021-12-12 01:02:17	38.67310	-97.47619	2.7	Saline
2021-12-12 01:10:29	38.66735	-97.47370	1.8	Saline
2021-12-12 01:17:03	38.67284	-97.47075	2.6	Saline
2021-12-12 02:09:22	38.66751	-97.47671	4.1	Saline
2021-12-12 02:18:02	38.66816	-97.48459	2.0	Saline
2021-12-12 02:45:00	38.66222	-97.46940	1.9	Saline
2021-12-12 03:29:44	38.67235	-97.50314	2.0	Saline
2021-12-12 04:16:38	38.64901	-97.46923	2.0	Saline
2021-12-12 05:15:56	38.64816	-97.49601	2.3	Saline
2021-12-12 08:35:42	38.67215	-97.47074	2.2	Saline
2021-12-12 08:40:19	38.66205	-97.47893	1.9	Saline
2021-12-12 09:27:17	38.66728	-97.47259	1.9	Saline
2021-12-12 11:55:45	38.66867	-97.48129	1.9	Saline
2021-12-12 12:04:10	38.66483	-97.47536	2.2	Saline
2021-12-12 13:51:39	38.66602	-97.48829	2.3	Saline
2021-12-12 16:13:27	38.66851	-97.47701	2.2	Saline
2021-12-12 23:19:36	38.67113	-97.47409	2.7	Saline
2021-12-13 04:57:43	38.67457	-97.48978	2.2	Saline
2021-12-13 17:29:53	38.66816	-97.47958	2.0	Saline
2021-12-14 06:38:10	38.66777	-97.46527	2.1	Saline
2021-12-14 07:48:23	38.66582	-97.48525	2.2	Saline
2021-12-14 12:22:24	38.66779	-97.45770	2.2	Saline
2021-12-14 13:35:03	38.66330	-97.46767	2.4	Saline
2021-12-14 22:02:29	38.66322	-97.47820	2.7	Saline
2021-12-15 09:58:20	38.66889	-97.47514	4.4	Saline
2021-12-15 10:08:11	38.66113	-97.47380	2.7	Saline
2021-12-15 10:16:21	38.66850	-97.46577	2.2	Saline
2021-12-15 11:14:06	38.66516	-97.48908	2.1	Saline
2021-12-15 12:35:04	38.67304	-97.49281	2.1	Saline
2021-12-15 13:23:01	38.65847	-97.45438	2.1	Saline
2021-12-15 14:34:59	38.67665	-97.48686	2.3	Saline
2021-12-15 14:54:59	38.66877	-97.47311	2.2	Saline
2021-12-15 15:03:07	38.68148	-97.47145	3.8	Saline
2021-12-15 18:17:48	38.67002	-97.49232	3.4	Saline
2021-12-16 02:09:46	38.63628	-97.45565	2.2	Saline
2021-12-16 03:16:18	38.66434	-97.45181	2.2	Saline
2021-12-16 10:39:49	38.66917	-97.49738	2.3	Saline
2021-12-16 19:54:24	38.66326	-97.50327	2.2	Saline
2021-12-16 21:07:13	38.65779	-97.47464	2.2	Saline
2021-12-17 00:18:41	38.64542	-97.46240	2.5	Saline
2021-12-17 14:23:42	38.67468	-97.47594	3.6	Saline
2021-12-17 14:53:33	38.66132	-97.48048	2.3	Saline
2021-12-17 14:57:04	38.66636	-97.48036	1.9	Saline
2021-12-17 17:10:05	38.65471	-97.50136	1.8	Saline

Table 1. Continued

Origin Time (UTC)	Latitude	Longitude	Magnitude	County
2021-12-17 20:32:56	38.67426	-97.47560	2.6	Saline
2021-12-18 00:56:47	38.64830	-97.52444	1.8	Saline
2021-12-18 01:23:56	38.67421	-97.49073	2.8	Saline
2021-12-18 15:21:37	38.66961	-97.48241	2.8	Saline
2021-12-19 08:07:02	38.64618	-97.48656	2.0	Saline
2021-12-19 18:04:01	38.67212	-97.48141	2.0	Saline
2021-12-20 14:21:24	38.67056	-97.49292	2.7	Saline
2021-12-20 19:58:57	38.66426	-97.44003	2.0	Saline
2021-12-21 00:54:54	38.68520	-97.46048	1.9	Saline
2021-12-21 01:42:19	38.68157	-97.44536	1.9	Saline
2021-12-22 01:50:31	38.66202	-97.46680	1.9	Saline
2021-12-22 07:25:08	38.67330	-97.48067	2.2	Saline
2021-12-22 18:08:04	38.65920	-97.46595	2.1	Saline
2021-12-26 10:54:39	38.68707	-97.51019	2.5	Saline
2021-12-26 11:08:46	38.67066	-97.48299	2.5	Saline
2021-12-26 12:06:39	38.68338	-97.49100	2.4	Saline
2021-12-26 12:51:48	38.64303	-97.52717	1.8	Saline
2021-12-26 17:47:07	38.68887	-97.55750	1.6	Saline
2021-12-26 21:16:35	38.66274	-97.48872	1.9	Saline
2021-12-27 05:23:39	38.66656	-97.50722	2.1	Saline
2021-12-27 05:51:30	38.65733	-97.45290	3.5	Saline
2021-12-27 06:06:24	38.66864	-97.45773	2.1	Saline
2021-12-27 06:56:42	38.65398	-97.49771	1.8	Saline
2021-12-27 07:59:02	38.63039	-97.50306	2.7	Saline
2021-12-27 09:58:14	38.64105	-97.49555	2.5	Saline
2021-12-27 14:02:55	38.65407	-97.50408	1.9	Saline
2021-12-27 15:50:44	38.67967	-97.54098	1.9	Saline
2021-12-28 08:34:00	38.66901	-97.47875	2.2	Saline
2021-12-28 11:32:55	38.66140	-97.52114	2.1	Saline
2021-12-28 12:33:52	38.65503	-97.44638	3.1	Saline
2021-12-28 18:37:59	38.66102	-97.51981	2.1	Saline
2021-12-29 13:53:35	38.64766	-97.51985	1.9	Saline
2021-12-29 18:45:56	38.64411	-97.50607	2.8	Saline
2021-12-30 14:49:57	38.65885	-97.46263	2.4	Saline
2021-12-31 04:00:37	38.66817	-97.45858	2.7	Saline
2021-12-31 20:04:49	37.43322	-97.92049	2.1	Kingman
2022-01-02 13:14:11	38.66458	-97.49358	2.2	Saline
2022-01-03 06:08:37	38.59822	-97.46437	2.7	McPherson
2022-01-03 14:57:26	37.30698	-97.71622	2.7	Sumner
2022-01-03 16:11:46	37.30560	-97.72718	2.0	Sumner
2022-01-05 22:55:11	37.31447	-97.71783	2.8	Sumner
2022-01-06 08:07:41	37.31295	-97.72448	2.4	Sumner
2022-01-06 10:24:38	37.31434	-97.72696	2.8	Sumner
2022-01-07 07:10:59	38.63827	-97.51060	2.6	Saline
2022-01-07 10:22:21	38.66917	-97.48787	2.3	Saline
2022-01-07 11:41:08	38.63354	-97.49778	2.2	Saline
2022-01-07 15:47:18	37.31828	-97.71907	2.1	Sumner
2022-01-09 11:58:10	38.65287	-97.48246	2.2	Saline
2022-01-10 14:35:39	38.66674	-97.49058	3.5	Saline
2022-01-11 09:27:37	38.66791	-97.49549	2.0	Saline
2022-01-12 15:33:10	38.68271	-97.51592	2.3	Saline
2022-01-14 23:42:43	38.66420	-97.46011	2.2	Saline
2022-01-15 00:35:16	38.67714	-97.49783	2.9	Saline
2022-01-15 09:29:08	38.64884	-97.44539	2.3	Saline
2022-01-17 01:38:23	38.65896	-97.53320	2.2	Saline
2022-01-18 19:28:19	38.66061	-97.45091	2.6	Saline
2022-01-20 13:52:02	38.67569	-97.49875	2.2	Saline
2022-01-20 14:21:19	38.66852	-97.51106	2.7	Saline
2022-01-25 20:20:05	37.31349	-97.72933	2.2	Sumner
2022-01-29 08:18:30	38.66950	-97.47871	1.9	Saline

Table 1. Continued

Origin Time (UTC)	Latitude	Longitude	Magnitude	County
2022-02-01 17:11:20	38.66800	-97.47511	2.6	Saline
2022-02-01 18:25:28	38.65487	-97.46728	2.8	Saline
2022-02-06 02:27:54	38.66887	-97.46774	2.4	Saline
2022-02-06 03:23:44	38.67028	-97.47601	2.1	Saline
2022-02-09 11:00:15	38.66845	-97.47636	2.3	Saline
2022-02-22 10:57:59	38.65688	-97.45647	2.7	Saline
2022-02-27 17:45:24	38.65778	-97.45214	2.1	Saline
2022-03-01 06:20:44	38.63490	-97.49458	2.1	Saline
2022-03-01 07:47:40	38.66253	-97.47105	2.1	Saline
2022-03-02 03:14:37	38.67823	-97.49475	2.1	Saline
2022-03-02 23:08:39	38.68342	-97.61393	2.1	Saline
2022-03-04 12:34:07	38.64319	-97.47857	2.2	Saline
2022-03-07 13:03:49	38.67256	-97.48961	2.4	Saline
2022-03-08 16:21:20	38.66557	-97.46183	1.9	Saline
2022-03-08 20:37:22	38.64977	-97.50700	3.3	Saline
2022-03-09 00:12:23	38.64745	-97.51869	1.9	Saline
2022-03-09 21:50:46	38.65917	-97.57557	1.9	Saline
2022-03-11 08:29:09	37.51219	-97.87141	2.0	Kingman
2022-03-11 17:41:21	38.61996	-97.59682	2.0	Saline
2022-03-12 16:23:40	38.61781	-97.59827	2.2	Saline
2022-03-13 17:22:19	37.31832	-97.72507	2.7	Sumner
2022-03-15 14:42:54	38.66319	-97.47838	2.2	Saline
2022-03-17 20:42:09	37.31672	-97.45345	2.0	Sumner
2022-03-18 18:18:27	38.68318	-96.89719	1.8	Morris
2022-03-19 01:03:58	37.51945	-97.75692	2.2	Sedgwick
2022-03-19 04:26:09	37.51724	-97.75138	2.7	Sedgwick
2022-03-19 04:27:14	37.51640	-97.75407	3.4	Sedgwick
2022-03-19 04:50:51	37.52549	-97.75051	2.0	Sedgwick
2022-03-19 12:26:21	37.51190	-97.74860	2.8	Sedgwick
2022-03-20 00:00:14	37.52091	-97.74859	3.7	Sedgwick
2022-03-20 00:05:18	37.52494	-97.76167	2.9	Sedgwick
2022-03-20 02:43:33	37.51644	-97.74801	2.5	Sedgwick
2022-03-20 08:31:16	37.50939	-97.75018	2.3	Sedgwick
2022-03-20 08:51:00	37.51348	-97.74706	2.8	Sedgwick
2022-03-20 15:40:32	37.51265	-97.74914	2.6	Sedgwick
2022-03-22 00:33:22	37.51019	-97.75558	3.1	Sedgwick
2022-03-22 04:03:26	38.64828	-97.53004	2.1	Saline
2022-03-22 06:13:16	37.51513	-97.74519	2.1	Sedgwick
2022-03-27 04:47:12	37.51455	-97.74386	2.4	Sedgwick
2022-03-27 12:11:33	38.64616	-97.52368	2.0	Saline
2022-03-27 21:33:16	38.65221	-97.50703	2.2	Saline
2022-03-28 08:25:38	38.67222	-97.48436	2.1	Saline
2022-04-09 15:09:35	38.48400	-97.41900	2.0	McPherson
2022-04-09 20:37:18	38.67300	-97.49200	2.0	Saline
2022-04-10 12:18:16	38.65200	-97.51100	2.1	Saline
2022-04-10 14:48:05	38.65300	-97.48800	2.3	Saline
2022-04-15 09:59:14	38.65387	-97.48776	2.9	Saline
2022-04-15 10:48:44	38.67400	-97.49600	2.0	Saline
2022-04-15 12:54:42	37.97600	-96.92700	2.1	Butler
2022-04-17 11:46:36	38.67500	-97.48600	2.1	Saline
2022-04-19 18:47:49	38.19300	-96.68600	2.1	Chase
2022-04-20 03:49:54	38.06000	-97.07500	2.0	Butler
2022-04-20 04:14:42	38.05300	-97.08300	2.0	Butler
2022-04-26 22:19:52	38.67400	-97.47400	2.1	Saline
2022-04-27 18:33:41	38.63800	-97.50100	2.2	Saline
2022-04-29 01:00:51	38.66400	-97.51700	3.0	Saline
2022-05-17 02:23:50	38.00900	-97.98200	2.6	Reno
2022-05-17 05:58:28	37.51200	-97.72700	2.1	Sedgwick
2022-05-21 23:21:59	38.67100	-97.45500	2.6	Saline
2022-05-22 19:41:39	38.42600	-97.18600	2.5	Marion

Table 1. Continued

Origin Time (UTC)	Latitude	Longitude	Magnitude	County
2022-05-22 21:00:07	38.66400	-97.47800	2.0	Saline
2022-05-24 06:20:15	38.65700	-97.50500	2.2	Saline
2022-05-30 17:21:26	38.62100	-97.52900	2.2	Saline
2022-05-30 18:06:39	38.66000	-97.49500	2.4	Saline
2022-06-03 00:28:12	38.67400	-97.48100	2.3	Saline
2022-06-04 16:23:50	38.66541	-97.46598	3.2	Saline
2022-06-04 21:47:50	38.67000	-97.50500	2.1	Saline
2022-06-06 17:42:37	38.66400	-97.43700	2.3	Saline
2022-06-28 22:24:02	38.45280	-98.03472	2.6	Rice

End of table

INTERESTING OBSERVATIONS AND SIGNIFICANT TRENDS

Regional Seismicity (M 2 or larger)

During the past year, 456 earthquakes M 2 or larger were recorded in Kansas (Figure 3). For the first time since 2016, the annual number of earthquakes increased, and the number of regional scale events (M 2 or larger) nearly doubled relative to the previous year (286 from July 2020 through June 2021). As in past years, the vast majority of these events either occurred in parts of the state where historic earthquakes occurred along prominent basement structures or where earthquakes were recorded in recent years. The only exception is a M 2.9 in Rice County, the first M > 2 earthquake in the county since a M 2.7 near the Rice–McPherson border in 1981. The most notable earthquake sequences this year occurred in southeast Saline County and included 19 M ≥ 3 events, which is unexpected based on the lack of historic earthquakes in this area.

South-Central Kansas (Sedgwick Basin)

More than a quarter of the regional-scale earthquakes (M 2 or larger) recorded by the KGS network were located in south-central Kansas (Figure 4). However, the rate of earthquakes in this area has dropped dramatically since the KGS network was installed in 2015. In Harper and Sumner counties, 27 M 2 or larger earthquakes were recorded during the past year, about the same as the previous reporting period and an overall decrease of more than 95% relative to 2015, during that same period (2015 to present) injection volumes in Harper County decreased more than 80%. Earthquake clusters generally occurred in areas where earthquakes were observed in previous years.

From 2015 to 2018, earthquakes migrated from the highly active zones of seismicity in Harper and Sumner counties progressively farther along structural trends into surrounding counties, including Sedgwick, western Butler, Kingman, and Reno counties. Earthquakes along these trends are most likely induced, triggered as a result of elevated pore pressure that effectively reduced frictional resistance along critically-stressed basement faults. Notable sequences of earthquakes within clusters near Hutchinson in 2019-2020 and Wichita in 2020-2021 may be influenced by nearby injection operations. Seismicity continues to occur at significantly lower rates this year within this zone of measured elevated pressures, with only four M ≥ 2 earthquakes near Hutchinson and three earthquakes of this size near Wichita.

Pratt Anticline

West of the Sedgwick Basin, elevated pore pressure was likely the cause of a significant increase in seismic activity in Barber, Comanche, and surrounding counties in 2015-2018. Earthquakes have continued to occur near the Pratt Anticline since that time, but at a much lower rate. Only four regional-scale earthquakes occurred in this area during the past year (Figure 5). This is noteworthy because 244 M 2 or larger earthquakes were recorded here in 2015-2018, an average of more than 60 events of this size per year. The large reduction in seismicity over the past three years is consistent with stabilizing formation pressures across the region and a drop in reported injection volumes.

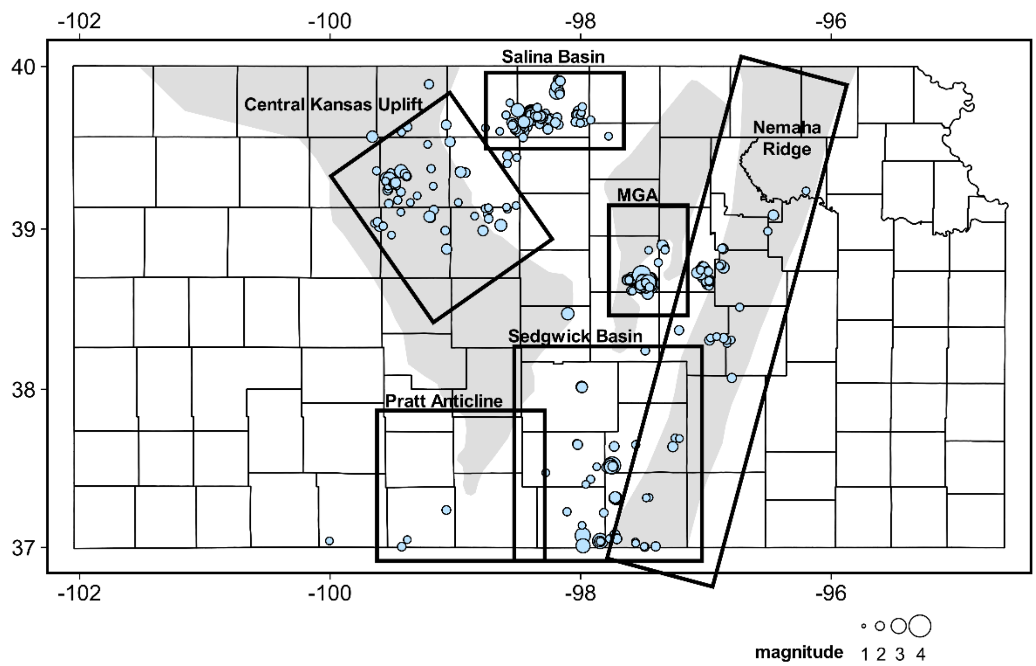

Figure 3. M 2 or larger earthquakes recorded in Kansas by the KGS seismic network from July 2021 through June 2022 (blue) superimposed on the prominent basement structures (gray).

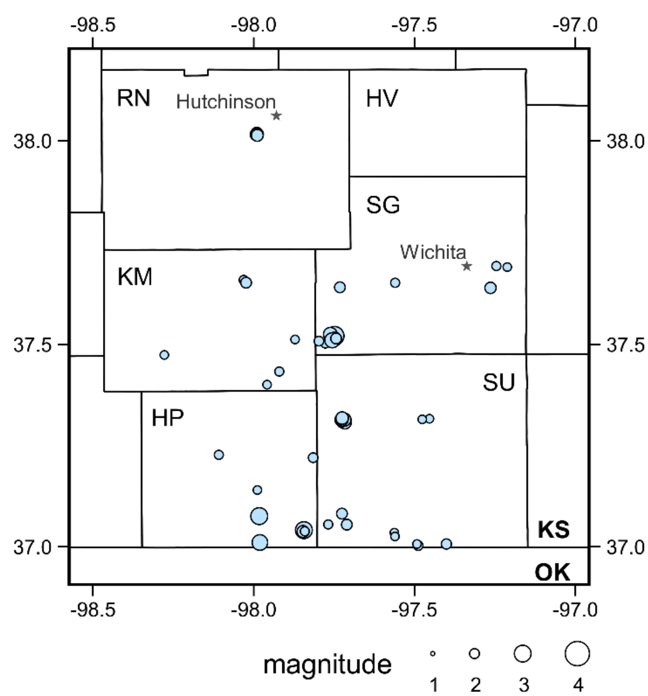

Figure 4. M 2 or larger earthquakes recorded in south-central Kansas from July 2021 through June 2022.

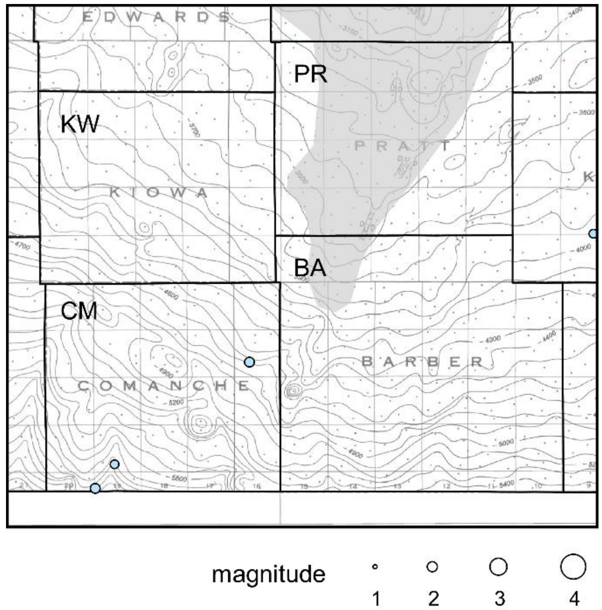

Figure 5. M 2 or larger earthquakes recorded in Kiowa, Pratt, Barber, and Comanche counties July 2021 through June 2022 superimposed on Precambrian structural contours (from Cole, 1976). The interpreted Pratt Anticline is shown in gray.

Central Kansas Uplift

Similar to the 2020-2021 reporting year, about 60 M 2 or larger earthquakes were recorded in areas affected by the Central Kansas Uplift (Figure 6). The largest event was a M 3.1 in southwest Rooks County about 10 mi from the location of a cluster of earthquakes that occurred in the late 1980s. These late 1980s earthquakes strongly correlated with nearby saltwater disposal operations and were suspected to have been induced (Armbruster et al., 1989). Several notable clusters of earthquakes have occurred in and around the Central Kansas Uplift in recent years. The spatial extent of the seismically active area migrated to greater distances over time, most notably from west to east across Russell County and continues to persist at generally low magnitudes (M less than 2). Although reliable pressure measurements are not available from wells that penetrate the full thickness of the Arbuckle Group (as in central and south-central Kansas), the persistent seismicity and progression of earthquakes is not behavior normally expected for natural seismicity and, thus, earthquakes in this area may be induced.

North-Central Kansas (Salina Basin)

Eighty-six M 2 or larger earthquakes were recorded in Smith, Jewell, and neighboring counties during the past year (Figure 7). The number of earthquakes in this area has progressively increased since early 2020 when there was a 4-month period from April to August of that year with no recorded earthquakes. Three M 3 or larger earthquakes occurred between 1928 and 2017, averaging one earthquake of this size every 44 years. Since 2017, more than three dozen M 3 or larger earthquakes occurred in Jewell County, averaging one earthquake of this size every 1-2 months. This trend continued with nine earthquakes with M greater than 3 this year. This significant increase in recurrence rate is not expected for natural earthquakes. At

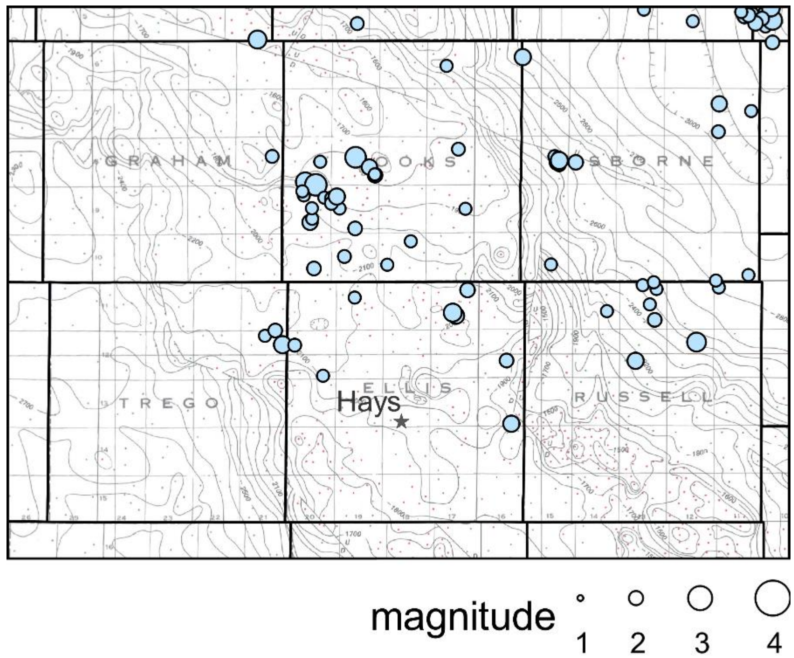

Figure 6. M 2 or larger earthquakes recorded near the Central Kansas Uplift from July 2021 through June 2022.

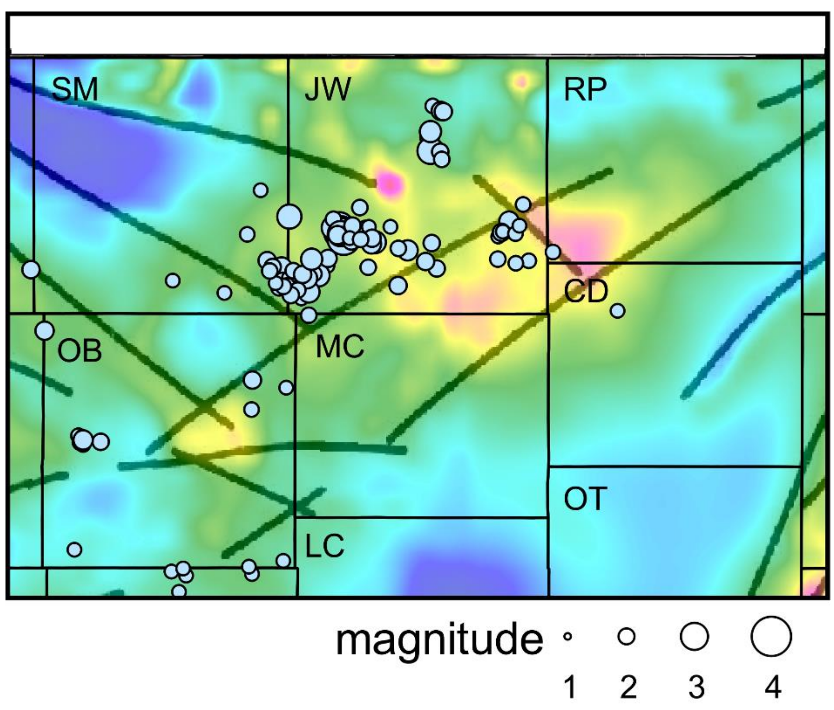

Figure 7. M 2 or larger earthquakes recorded in the Salina Basin from July 2021 through June 2022 superimposed on the aeromagnetic map (Xia et al., 1995) and interpreted magnetic lineaments (Yarger, 1983).

this time, the trigger for these earthquakes remains unclear, but they appear to be consistent with lineaments interpreted on aeromagnetic data.

Midcontinent Geophysical Anomaly

The Midcontinent Geophysical Anomaly (MGA, the largest positive gravity anomaly in North America) is interpreted to be the result of a thick sequence of mafic igneous rocks that formed during major late Precambrian rifting as part of the Midcontinent Rift System. Two ongoing clusters of earthquakes have been recorded along the southeastern margin of the MGA since the KGS network was installed in 2015. The rate of M 2 or larger earthquakes (Figure 8) increased five-fold this year with 189 earthquakes of this size (compared to only 37 the previous reporting year). The majority of these events are foreshocks or aftershocks in earthquake sequences that occurred in October and December 2021. These events are discussed in greater detail in the section on local seismicity near McPherson County member wells.

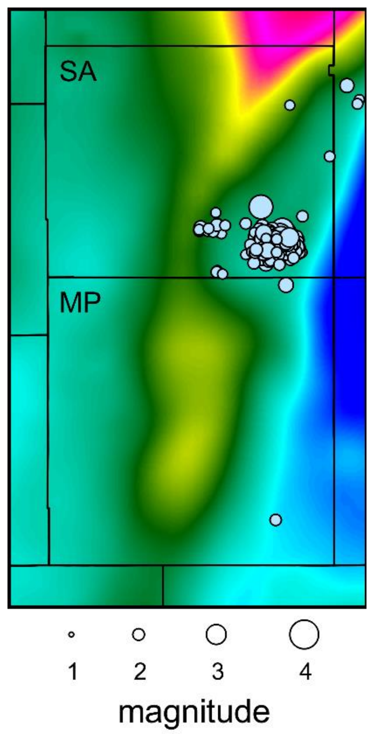

Figure 8. M 2 or larger earthquakes recorded near the Midcontinent Geophysical Anomaly from July 2021 through June 2022 superimposed on the gravity anomaly map of Kansas (Xia et al., 1995).

Nemaha Ridge

The Nemaha Ridge is one of the most prominent crustal features in Kansas, extending across the state with a northeast-southwest orientation. The Nemaha Ridge formed during post-Mississippian uplift of Precambrian age granite. A system of normal and reverse faults on the eastern margin of the Nemaha Ridge forms the Humboldt Fault Zone. Transform faults with a northwest-southeast trend intersecting the Nemaha Ridge represent a pre-Phanerozoic crustal extension associated with the Midcontinent Rift System. Dozens of historic earthquakes have been felt or recorded along the Nemaha Ridge, including an estimated M 5.2 near Wamego in 1867.

Fifty-one M 2 or larger earthquakes were recorded during the reporting period along the Nemaha Ridge ranging from Riley County to Marion County (Figure 9), which is about the same as the previous year. This year, seismic activity was scattered along the Ridge in areas where clusters have previously been observed. The most prominent cluster was in southeast Dickinson, where earthquakes have persisted since late 2018. Only one M 3 or larger event occurred this year (a reduction from six last year). The rate of M 3 or larger earthquakes in this area is unusual relative to more than a decade of monitoring in the 1970s and 1980s and the primary trigger for these events is unclear at this time, but the increase in seismic activity may represent a natural temporal fluctuation in seismic rate.

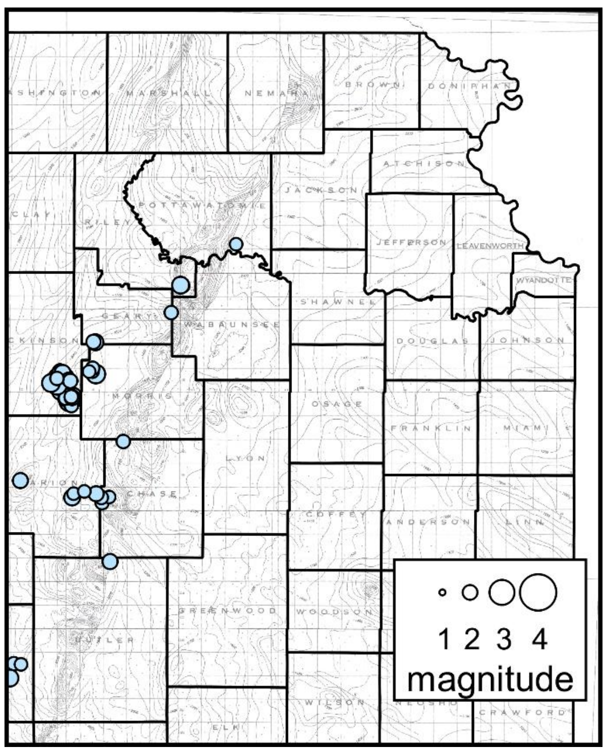

Figure 9. M 2 or larger earthquakes recorded along the Nemaha Ridge from July 2021 through June 2022 superimposed on Precambrian structural contours (from Cole, 1976).

Local Seismicity within 20 mi of Member Wells

Together with regional-scale felt events, analysis of events well below M 2 greatly improves our ability to interpret earthquakes relative to structures and evaluate possible causal factors. Sub M 2 events provide opportunities to forecast once the recursion relationship in specific areas can be accurately calculated for the current pressure regime. During the past year, 1236 microearthquakes (M less than 2) were recorded by the KGS seismic network (with enhanced sensitivity and improved location accuracy possible with the addition of CSTS stations) (Figure 10). Similar to regional scale earthquakes, the overall number of micro-earthquakes increased this year for the first time after steadily decreasing since 2015. Micro-earthquakes make up 72% of the events logged into the earthquake catalog last year. Of the entire catalog at all magnitudes, 157 earthquakes (the smallest number since recording began) were mapped within 20 mi of Tier 1 member wells (Appendix B).

Uniquely locating the epicenter of an earthquake requires detecting P- and/or S-waves at three or more stations. Subnetwork events are defined as earthquakes (typically with magnitudes less than M 1) that are only recorded on a single or at most two stations and, therefore, the epicenter location cannot be determined uniquely. Rather, the epicenter exists somewhere on a circle centered on the seismic station with radius equal to the calculated distance to the earth-quake epicenter. The magnitude of a subnetwork event is estimated from the coda, or duration—the time from the first P-wave arrival until the energy is approximately equal to or drops below the noise floor at that time and station (background noise usually based on pre-event noise levels). There were 294 subnetwork events recorded at CSTS stations (Appendix C), a decrease of 70% relative to last year. Some events may have an anthropogenic origin (for example, underground blasting). However, the majority of these subnetwork events are low-energy micro-earthquakes that provide valuable insight into the relative stability and stress conditions of faults in proximity to the station (within about 12 mi) and the member facility.

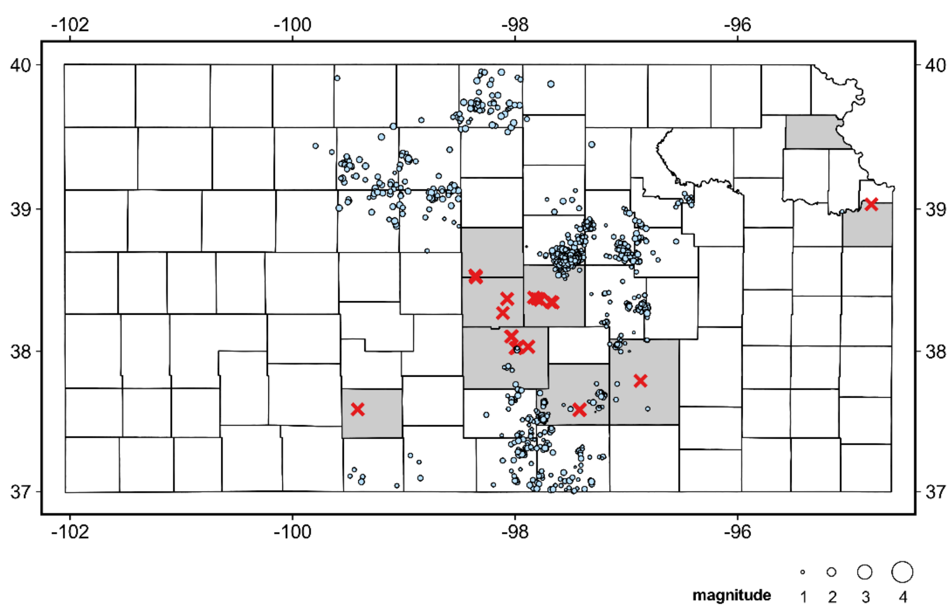

Figure 10. Microearthquakes (M less than 2) recorded in Kansas by the KGS seismic network from July 2021 through June 2022. Gray shading indicates counties with CSTS member wells (red Xs).

In this section, seismicity at all magnitudes (including both uniquely located events and subnetwork events) and relevant basement structures are evaluated in each of the nine counties with Tier 1 member wells.

Kiowa County

Similar to last year, no earthquakes were mapped within 20 miles of the Kiowa County member well (Figure 11a). However, the number of subnetwork events increased from only one last year to 17 this year (Figure 11b). The nearest uniquely located earthquakes were 30 mi or more away in neighboring Comanche and Barber counties. These events were sparse and low-magnitude, and the majority occurred at about the same locations as clusters of earthquakes recorded during previous reporting periods. The lack of mapped earthquakes in Kiowa County is consistent with the overall stabilizing of pressures in south-central Kansas as observed in Harper, Sedgwick, and Kiowa county wells. The increase in low-magnitude earthquakes (subnetwork events) raises the likelihood of a larger, potentially felt event in the future.

Rice and Ellsworth Counties

One earthquake was located within 20 mi of the member wells in Rice and Ellsworth counties (Figure 12a). This M 2.9 event is the first earthquake recorded in Rice County since a M 2.7 in 1981. The number of subnetwork events recorded this year at Rice County stations RC02 and RC03 is consistent with the long-term average (Figure 12b). However, more than double the average number of subnetwork events were recorded last year at station RC02 with epicentral distances averaging about 5 mi. This distance is consistent with the location of the epicenter of the M 2.9 earthquake near a mapped fault on the margin of the Geneseo Uplift, an eastern lobe of the Central Kansas Uplift and the predominant basement structure in Rice County (Berendsen and Blair, 1986). The 2020-2021 microearthquakes may have been precursors to the later felt event. Formation pressures (discussed in a later section) appear to be somewhat elevated in Rice County, but it is unclear if the pressure change is large enough to trigger earthquakes. At this time, it appears that the Rice County seismicity is likely the result of natural crustal stresses. However, it does indicate that this area has active faults that may be susceptible to induced seismicity if formation pressures were to further rise.

(a)

(b)

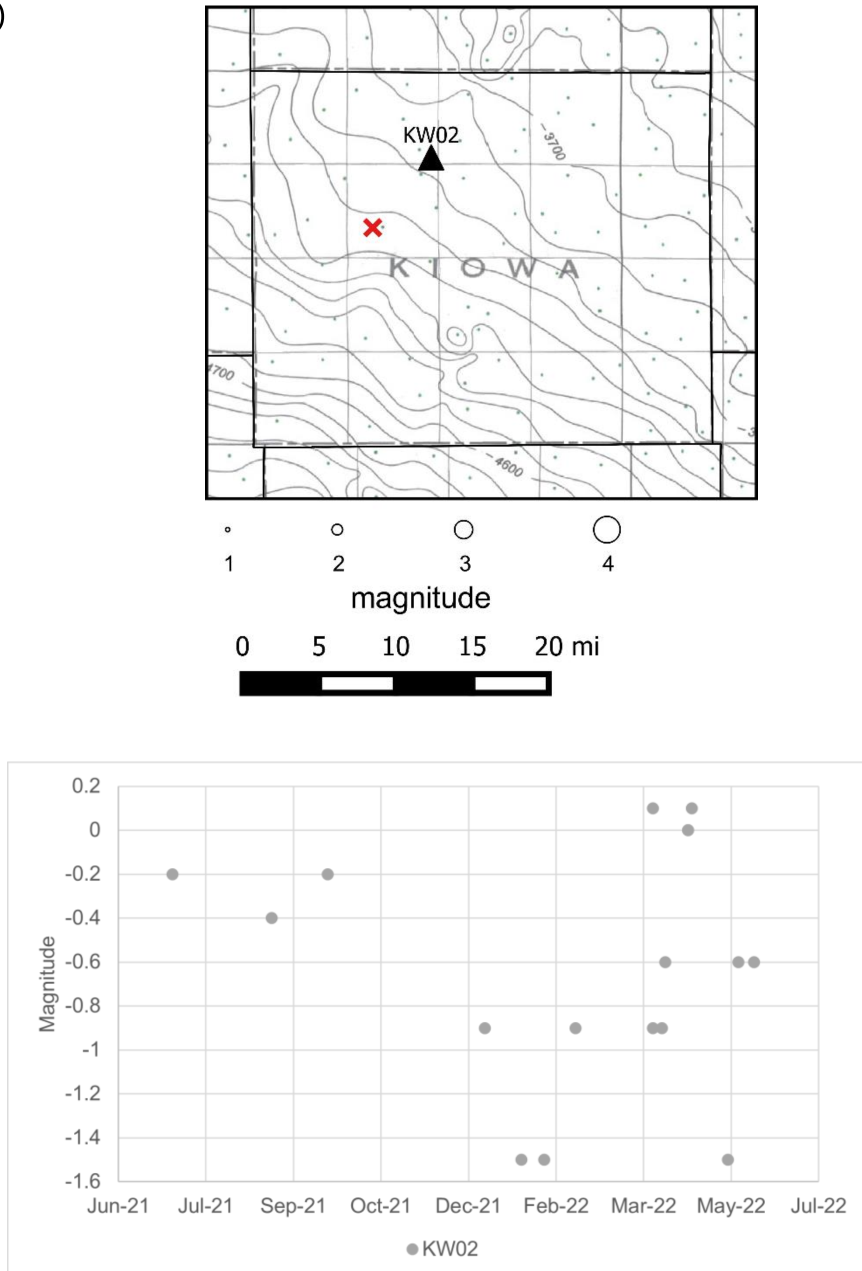

Figure 11. (a) Earthquakes recorded in Kiowa County from July 2021 through June 2022 superimposed on Precambrian structural contours (from Cole, 1976) and inferred Pratt Anticline at the southern end of the Central Kansas Uplift (gray). CSTS member wells and stations in the CSTS network are indicated by a red X and black triangle, respectively. (b) Scatter plot of subnetwork events recorded within 12 mi of CSTS stations.

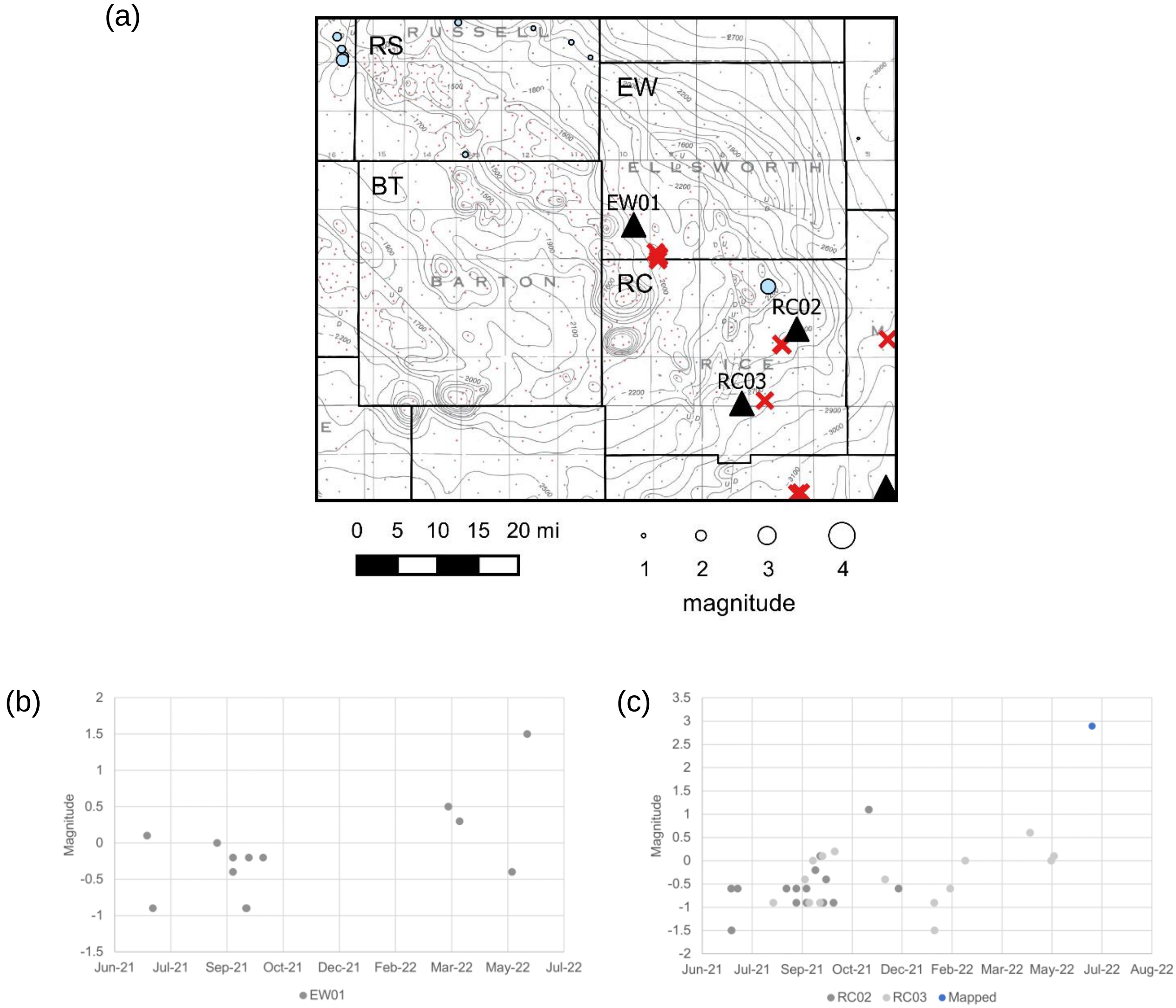

Figure 12. (a) Earthquakes near Rice and Ellsworth counties from July 2021 through June 2022 superimposed on Arbuckle Group structural contours (from Berendsen and Blair, 1986). CSTS member well and station in the CSTS network are indicated by a red X and black triangle, respectively. Scatter plots of subnetwork events recorded within 12 mi of CSTS stations in (b) Rice County and (c) Ellsworth County.

Station EW01 is located in the southwest corner of Ellsworth County. An average of 5 subnetwork events per year were detected at EW01 from 2017 when recording began to 2019. Thirteen subnetwork events with $M \leq 1.5$ were recorded at an average epicentral distance of 4 mi were recorded this year (Figure 12bc). Seismic activity in this area largely appears to represent continued low-energy movement on faults that produced nearby historic earthquakes. It is possible that the increase in subnetwork events both this year and last year simply represents a natural variability in earthquake rates. However, the generally west to east progression of possibly-induced earthquakes across neighboring Russell County (Buchanan et al., 2021) may indicate pore pressure changes could be migrating into Ellsworth County and triggering low-magnitude earthquakes.

McPherson County

Seismic activity within 20 km of member wells in McPherson County was primarily concentrated near the McPherson-Saline County border (Figure 13). These events occur near the eastern margin of the Midcontinent Geophysical Anomaly (MGA) along and east of the Salina Fault in Saline County. Seismicity in this area has been ongoing since installation of the KGS seismic network in 2015 with about 100 M 2 or larger earthquakes cataloged from 2015-2020. Seismic activity increased dramatically this year with 187 M 2 or larger earthquakes, including three M 4 or larger. As mentioned in the previous section, many of these events are foreshocks or aftershocks of larger main shocks. Given the lack of recorded earthquakes in Saline County prior to 2015, the probability of such a dramatic change in seismicity is extremely low for natural earthquakes. Arbuckle Group formation pressures measured in McPherson County have been steadily rising since 2014 and are currently about 30 psi greater than historic pressures (Figure 14). The rise in pressure appears to be related to pressure diffusion from high-volume disposal near the southern Kansas border. Although there are no pressure measurements for the Arbuckle or basement in Saline County, it is reasonable to assume pressures have risen here as well. Without pressure data or detailed (e.g., daily metered) disposal volume data from Saline County wells, the exact cause or triggering mechanism of these earthquakes remains unclear.

Historically, seismicity within 20 mi of McPherson County member wells is extremely sparse and persistent seismicity in this area would not be expected. To date, only a few earthquakes have occurred in McPherson County outside of the cluster at the northern county line. A M 2.2 earthquake occurred in November 2021 in the southeast corner of the county 11 mi or more from member wells. Five microearthquakes occurred at the same location in 2019 and early 2021, indicating the presence of a seismically active structure. An earthquake of this size subsequently occurring is not surprising based on recurrence rates of natural earthquakes. In the absence of other influences (e.g., pressure changes from injection operations), earthquakes are likely to continue at this location at similar rates and magnitudes.

Station MP01 is bounded to the west and east by northeast trending faults mapped in Precambrian and/or Arbuckle Group rocks associated with the Midcontinent Rift System. Forty-two subnetwork events were recorded at MP01 with magnitudes ranging from -1.5 to 0.4 (Figure 13b). These events occurred at various times of day and most occurred at an epicentral distance of about 5 mi. This distance is consistent with the location of a M 2.6 earthquake that occurred on November 3, 2014. The average rate of subnetwork events at MP01 is about a dozen events per year and, therefore, this year's rate is about three times greater than average but consistent with last year. It is unclear at this time if the rate increase represents a natural fluctuation or if it suggests anthropogenic influence. This cluster bears special attention including enhanced comparisons between diffusivity, injection rates and volumes, and pressures in member wells.

Thirty-seven subnetwork events were recorded at station MP02 with magnitudes ranging from -1.5 to 0.4 (Figure 13b). The rate of subnetwork events at MP02 is generally higher than other stations with about two dozen per year, with the number this year fewer than last year. These events occurred at epicentral distances ranging from 0 to 7 mi. MP02 is bounded to the west by a system of faults associated with the Voshell Anticline, to the southeast by the Halstead Fault, and is surrounded by a number of anticlinal and synclinal structures. The grouping of mapped earthquakes in the southeast corner of the county (described above) is about 6 mi from MP02. Therefore, these events are likely occurring on seismically active structures responsible for the larger mapped earthquakes.

Clustering of earthquakes and persistent seismicity can be an indicator that elevated pore pressures are influencing seismicity in McPherson and neighboring Saline counties. With a b-value of 1 this cluster is producing earthquakes with magnitudes consistent with the Gutenberg-Richter relationship, which was formulated based on naturally occurring earthquakes. Several dozen Class II saltwater disposal wells operate in the immediate vicinity of the McPherson–Saline earthquakes, more than 10 of which terminate in the Arbuckle Group. However, these wells are relatively low-rate, with the highest-rate well injecting less than 3,000 bbl/day. Therefore, it is unclear what role nearby disposal may play in the elevated seismic activity. A consistent question arising from arbitrary determinations of low versus high rates and potential to induce seismicity, is this: how much injected volume will be necessary to alter pressures sufficiently to surpass the triggering threshold.

(a)

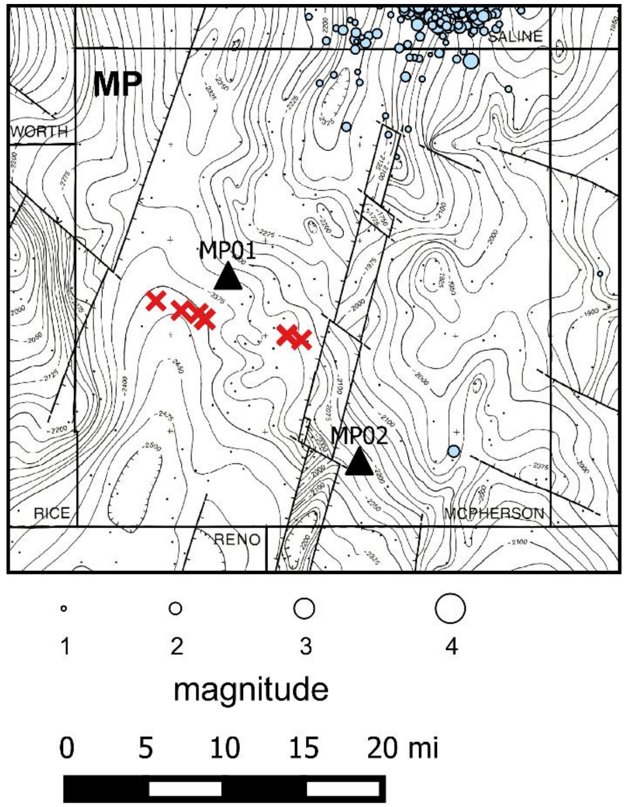

(b)

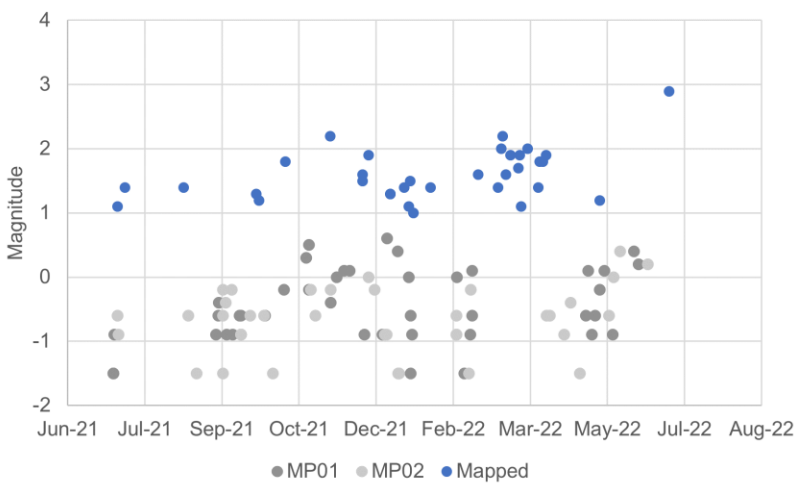

Figure 13. (a) Earthquakes recorded in McPherson County from July 2021 through June 2022 superimposed on Arbuckle Group structural contours (from Berendsen and Blair, 1986). CSTS member wells and stations in the CSTS network are indicated by a red X and black triangle, respectively. (b) Scatter plot of earthquakes (blue) recorded within 20 mi of member wells and subnetwork events (gray) recorded within 12 mi of CSTS stations.

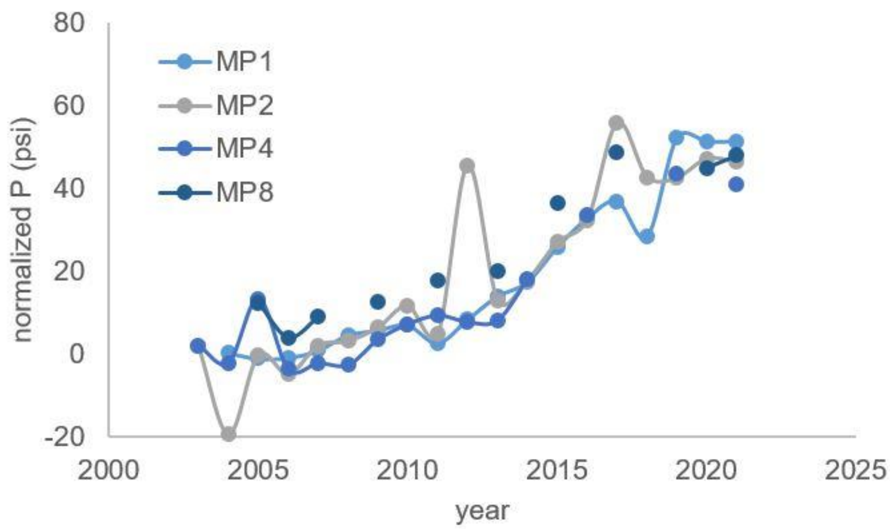

Figure 14. Change in formation pressure relative to historic values in Class I wells in McPherson County.

Reno County

Only 16 earthquakes were recorded in Reno County during the current reporting period. Five microearthquakes (M ≤ 1.7) were located in the southern half of the county near previously-recorded clusters, and 11 earthquakes were recorded in the Hutchinson cluster (Figure 15a). This is a remarkable decrease in seismic activity, considering that an order of magnitude more earthquakes (133) were recorded in Reno County during the previous reporting period. The decrease in seismic activity is consistent with stabilizing or possibly decreased pore pressures measured during 2020, while injection volumes remained relatively consistent in Reno County over the last decade while total volumes dropped across the state. The largest events recorded near Hutchinson this year were a M 2.7 on July 17, 2021, and M 2.6 on May 17, 2022. The remaining Hutchinson earthquakes largely occurred as fore- or aftershocks in the earthquake sequences of these two main shocks.

Station RN01 is located 2-3 mi northwest of the Hutchinson earthquakes. Forty-two subnetwork events were recorded at RN01 with magnitudes ranging from -1.5 to 0.6 (Figure 15b). These events occurred regularly throughout the year but tapered off from October to December 2021, with only 3 subnetwork events during that time. This is a substantial decrease from the more than 400 subnetwork events/year average since 2017, and is consistent with the overall drop in earthquake rate in the Hutchinson cluster since January 2020. The estimated epicentral distances of nearly all these events is about 4 mi. Although this is slightly larger than the 2.8 mi distance to the center of the mapped Hutchinson earthquakes, these microearthquakes almost certainly originate from the same fault or set of faults. The epicentral distance was calculated assuming a fixed earthquake depth of 3 mi, which is a common assumption used to locate earthquakes in the midcontinental U.S. Earthquakes are likely occurring on faults within the shallow Precambrian basement, which is at a depth of about 1 mi in this part of Reno County. Recalculating the epicentral distance using a depth of 1 mi results in an average distance of 3 mi, which is consistent with the location of the swarm of earthquakes located by the KGS regional seismic network. These events provide confidence in the suggestion that the Hutchinson earthquakes are occurring in the shallow basement.

Similar to previous years, 22 subnetwork events were recorded at station RN03. Although the Hutchinson Fault runs NE-SW through the northeast corner of Reno County and east of the City of Hutchinson, no mapped earthquakes have been recorded along that fault since monitoring began in 2017. The subnetwork events occurred at distances ranging from 1-9 mi, which is consistent with the Hutchinson fault. Subnetwork events recorded at RN03 may be microearthquakes occurring along this structure.

(a)

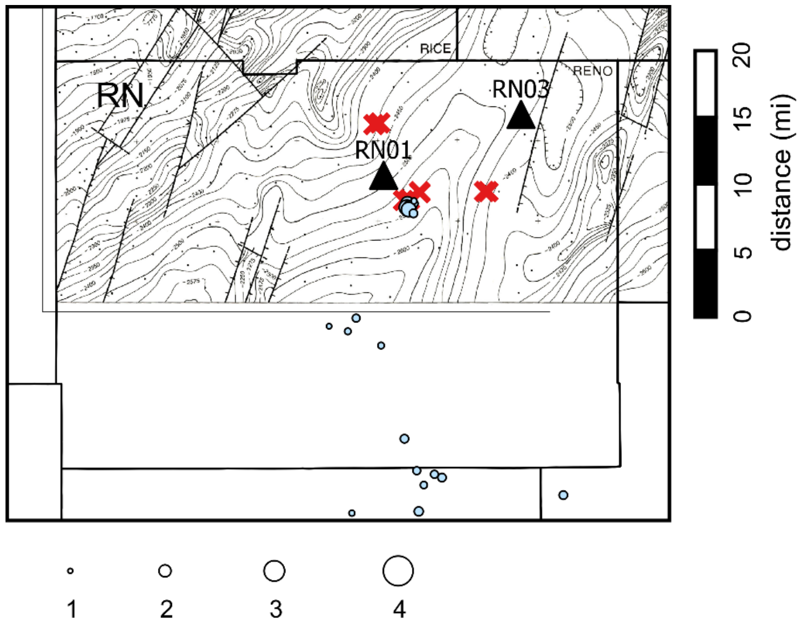

(b)

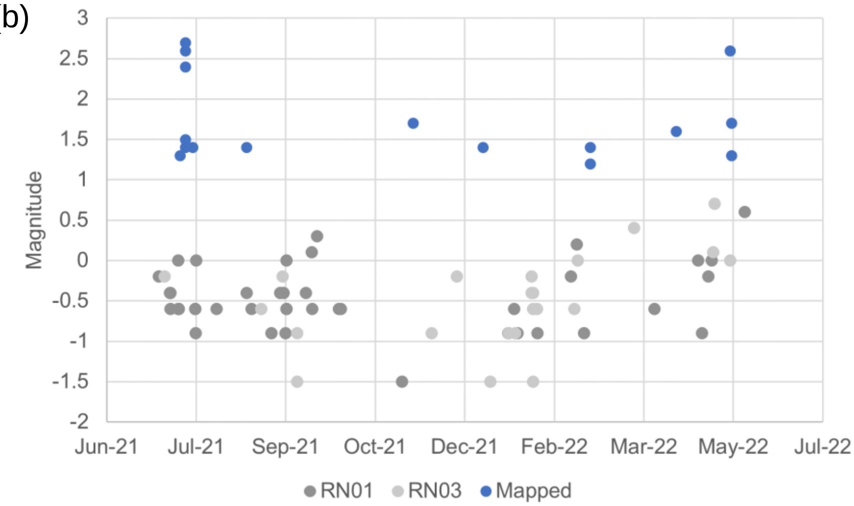

Figure 15. (a) Earthquakes recorded in Reno County from July 2021 through June 2022 superimposed on Arbuckle structural contours (from Berendsen and Blair, 1986). CSTS member wells and stations in the CSTS network are indicated by a red X and black triangle, respectively. (b) Scatter plot of earthquakes (blue) recorded within 20 mi of member wells and subnetwork events (gray) recorded within 12 mi of CSTS stations

Sedgwick County

Last reporting year, a cluster of nearly 150 earthquakes occurred in east Wichita, including multiple distinct sequences with 25 M 2 and 11 M 3 earthquakes. Unlike prior earthquakes near Wichita, the events had an abrupt onset and increasing energy release from November 26 to December 30, 2020. Given the stabilizing and possibly decreasing formation pressures in Sedgwick County, these earthquakes were somewhat unexpected. This year, the earthquake rate near Wichita dropped considerably with only 34 earthquakes, the largest of which was a M 2.5. Consistent with years prior to 2020 and 2021, seismic activity continued in the Cheney area with about 40 earthquakes, the largest of which was a M 3.7. While formation pressures in this area remain elevated well above historic levels, earthquakes will likely persist and seismically active structures will continue to be sensitive to pressure fluctuations (e.g., from local injection operations).

Similar to last year, 29 subnetwork events were recorded at station SG02 with magnitudes ranging from -1.5 to 0.3 (Figure 16b). Unlike previous years, the majority of these events occurred at epicentral distances within 3 mi of the station (about the distance to a group of nearby Class I wells. Half of these events occurred within a 24 hour period (on January 2, 2022). This date does not correspond to anomalous disposal volumes in nearby wells or any larger earthquakes (local or distant). Subnetwork events are likely occurring on faults associated with the Valley Center anticline as a result of elevated formation pressures. Due to lack of correlation with nearby disposal volumes or earthquakes, it is unclear if these events were triggered or simply a result of natural crustal stress release.

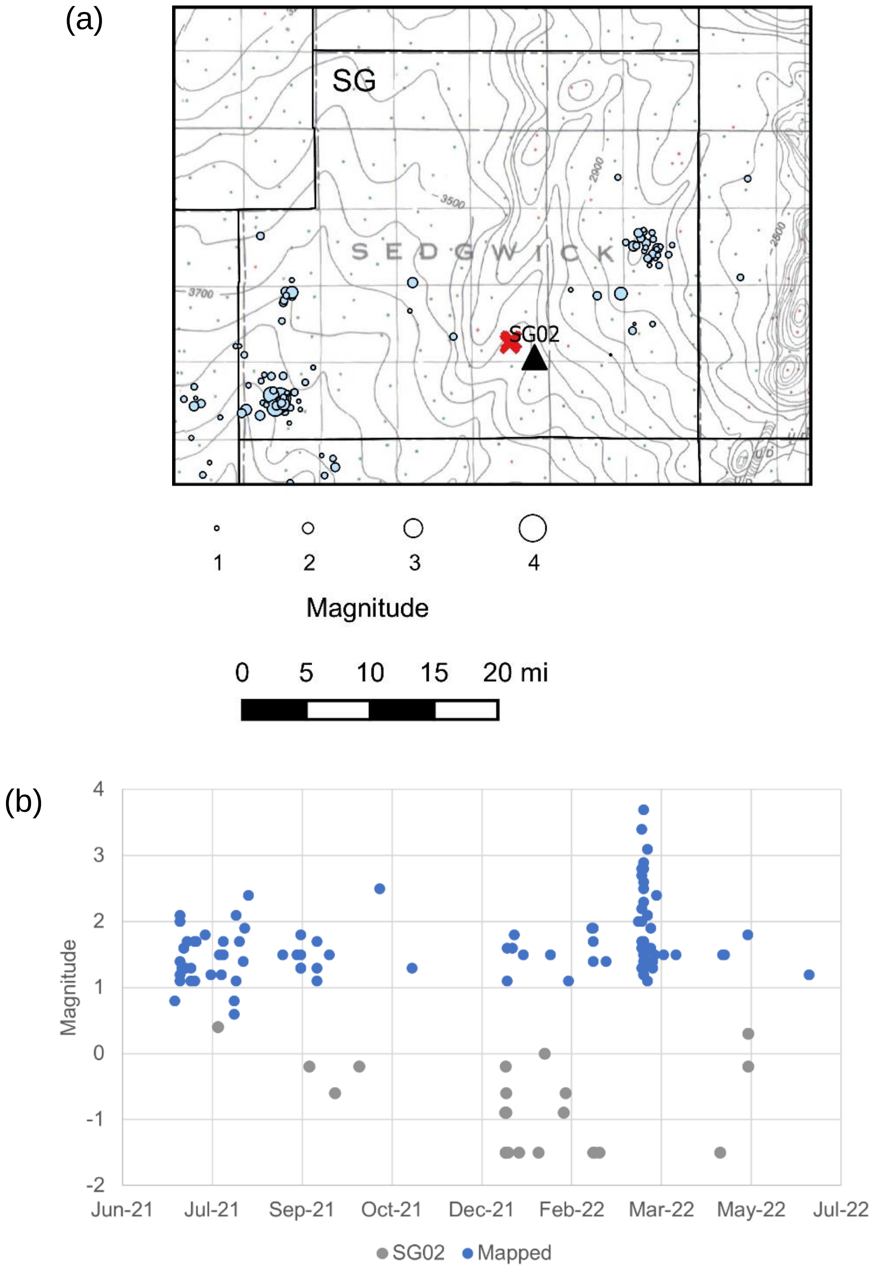

Figure 16. (a) Earthquakes recorded in Sedgwick County from July 2021 through June 2022 super-imposed on Arbuckle Group structural contours (from Berendsen and Blair, 1986). CSTS member wells and stations in the CSTS network are indicated by a red X and black triangle, respectively. (b) Scatter plot of earthquakes (blue) recorded within 20 mi of member wells and subnetwork events (gray) recorded within 12 mi of CSTS stations.

Butler County

Eleven earthquakes were mapped within 20 mi of the Butler County member well this year (Figure 17). The majority of these events occurred in east Wichita near the Sedgwick–Butler County line, discussed in the previous section. A few sparse microearthquakes occurred in areas of Butler County where earthquakes have been observed previously. There was a threefold increase in subnetwork events recorded at station BU02. The majority of these events occurred within 2 mi of the station and do not correlate with a larger main shock. Interestingly, the majority of the events occurred in two distinct sequences on January 2 and February 23, 2022. Note that a distinct sequence of subnetwork events also occurred on station SG02 on January 2, 2022, and began at nearly the same time (2:55 am at SG02 and 3:20 am at BU02). It is possible for the passing seismic waves from a distant earthquake to trigger earthquakes in separate counties. However, such seismic waves are not evident on the continuous data at this time, and no events large enough to trigger earthquakes in Kansas are in the national and global catalogs. Therefore, it may simply be a coincidence that microearthquake sequences occurred in adjacent counties at similar times.

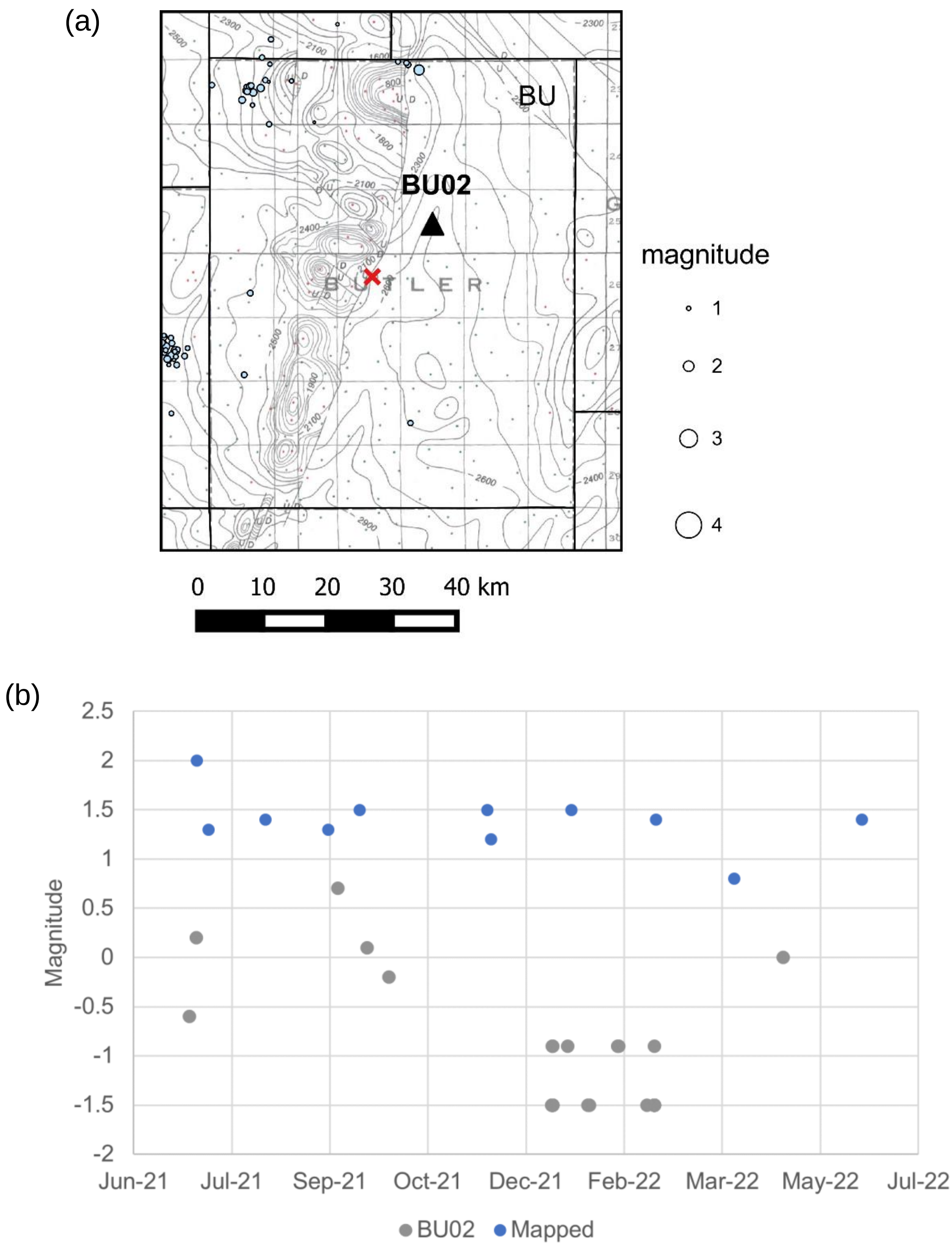

Figure 17. (a) Earthquakes recorded in Sedgwick County from July 2021 through June 2022 superimposed on Arbuckle Group structural contours (from Berendsen and Blair, 1986). CSTS member wells and stations in the CSTS network are indicated by a red X and black triangle, respectively. (b) Scatter plot of earthquakes (blue) recorded within 20 mi of member wells and subnetwork events (gray) recorded within 12 mi of CSTS stations.

Johnson and Atchison Counties

One earthquake was mapped within 20 mi of the Johnson County member well (Figure 18a). This event was a M 1.3 in neighboring Douglas County, the first earthquake recorded in the county since a M 1.8 in 1980. Seven subnetwork events were recorded at station JO01 in two spatial grouping at epicentral distances of ~2 mi and 10 mi; three subnetwork events were recorded within 5 mi of station AT01 (Figure 18b). These observations are more or less consistent with previous years and the mapped earthquake in Douglas County is not unexpected given the history of seismicity. A very low earthquake rate in this region is unsurprising given the stable tectonic regime and limited number of historic earthquakes recorded here.

(a)

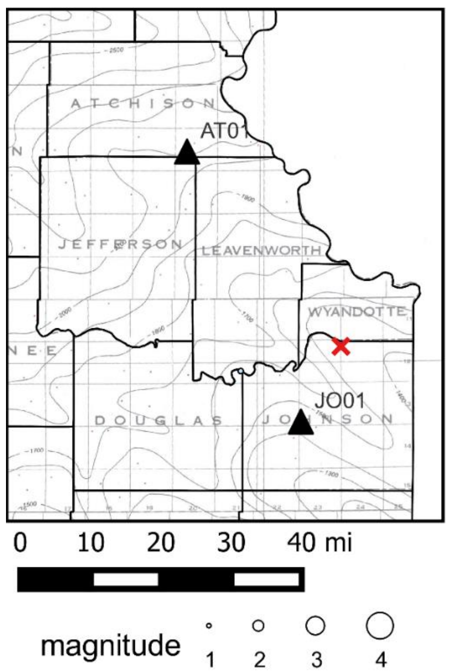

(b)

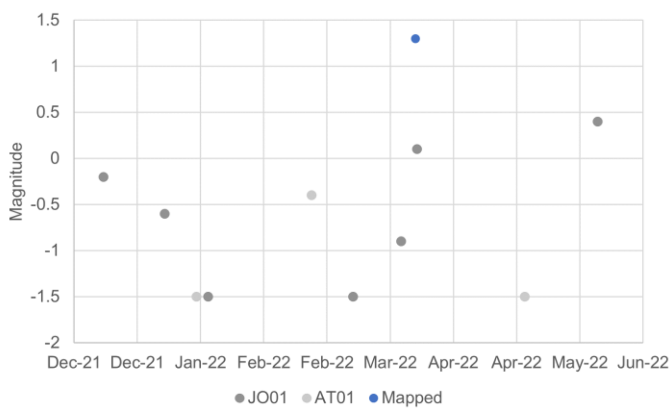

Figure 18. (a) Earthquakes recorded in Johnson and Atchison counties from July 2021 through June 2022 superimposed on Arbuckle Group structural contours (from Berendsen and Blair, 1986). CSTS member wells and stations in the CSTS network are indicated by a red X and black triangle, respectively. (b) Scatter plot of subnetwork events recorded within 12 mi of CSTS stations.

DISCUSSION

The Arbuckle Group is a deep aquifer that serves as the injection zone for thousands of Underground Injection Control (UIC) wells in Kansas and neighboring Oklahoma. Widespread seismic activity across central Oklahoma and south-central Kansas is primarily attributed to elevated pore pressures along critically-stressed faults in the hydraulically-connected basement underlying the Arbuckle Group. As injection volumes in south-central Kansas decreased over the past five years, pressures in south-central Kansas began to stabilize in 2016 and the earthquake rate likewise began levelling off (Figures 19 and 20). In 2021 (the most current year with complete pressure data), pore pressures within the Arbuckle Group (and thus, basement where hydraulically connected) remain elevated at levels above the earthquake triggering threshold as defined as pre-2012 levels, but appear to be gradually declining in some areas while increasing in others (Figure 21). Therefore, earthquakes will likely persist as crustal stresses continue to load near-critical faults properly aligned with the stress field. Furthermore, with most of the areas of the state that have been seismically active over the last decade retaining formation pressures above triggering thresholds, injection practices that produce even small pressure fluctuations or pulses may contribute to anthropogenically trigger earthquakes on nearby faults, as may have been the case in Wichita area last year and Hutchinson a couple years ago.

Although most earthquakes correlate with prominent basement structures, the localized spatial trends are somewhat puzzling. For example, induced seismicity in Sumner County largely occurred in northeast trending lineaments parallel to the western margin of the Nemaha Ridge and other structural trends (e.g., Midcontinent Rift System). Seismicity along these lineaments abruptly terminates in northern Sumner County even though these basement structures are mapped to extend further to the northeast. From a structural perspective alone, it is unclear why this would be the case if these lineaments are contiguous as mapped. Correlations with patterns in magnetic anomalies may shed some light on these observations. The aeromagnetic map of Kansas reveals changes in magnetic susceptibility of deep rocks and, therefore, changes in basement rock type (Yarger, 1989). Seismicity in south-central Kansas in general occurs in areas with larger magnetic field values and thus rock types with greater magnetic susceptibility (Figure 22). Earthquake lineaments tend to truncate at or follow boundaries of lower magnetic susceptibility and, thus, different basement rock type. Similar observations were made in Oklahoma, although on a smaller local rather than regional scale. Earthquake sequences in Oklahoma appear to terminate near the edges of intrusions, either due to fault termination or changes in permeability that inhibit fluid flow (Shah and Crain, 2018). More research is necessary to better understand this correlation in Kansas.

This apparent connection between earthquake epicenters and magnetic susceptibility has strong implications with respect to localized injection and the associated changes in Arbuckle fluid pressures. With the exception of around 10 earthquakes within the Wichita Low (this term is based on the large areal extent and anomalously low susceptibility of the rocks) the boundary of the low appears to designate a relatively abrupt transition from areas with high seismicity along multiple trend lines to areas almost void of located earthquakes. The exception to this observation is the relatively narrow band of seismicity coincident with the Humboldt Fault that trends NE/SW along the east side of the Nemaha Ridge. Based on the correlation of basement rocks with magnetic properties, basement rock or structural characteristics of basement rocks in central Kansas generally control the seismicity that has increased in direct correlation with increased annual volumes of fluid injected into the Arbuckle formation.

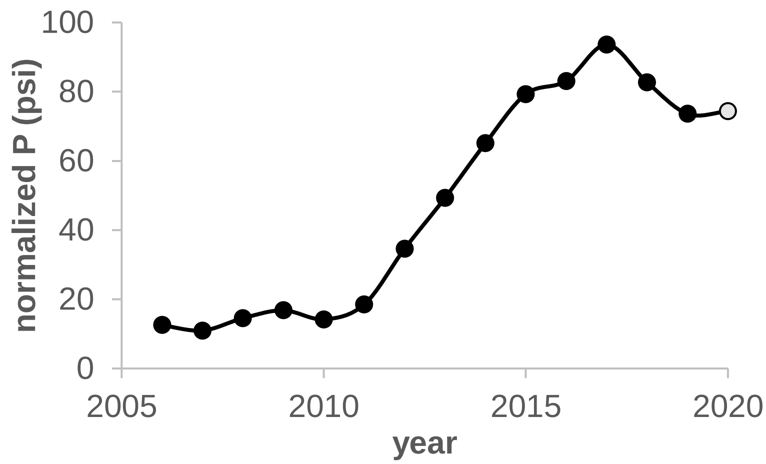

Figure 19. Arbuckle Group pore pressure reported for the Class I facility in Harper County.

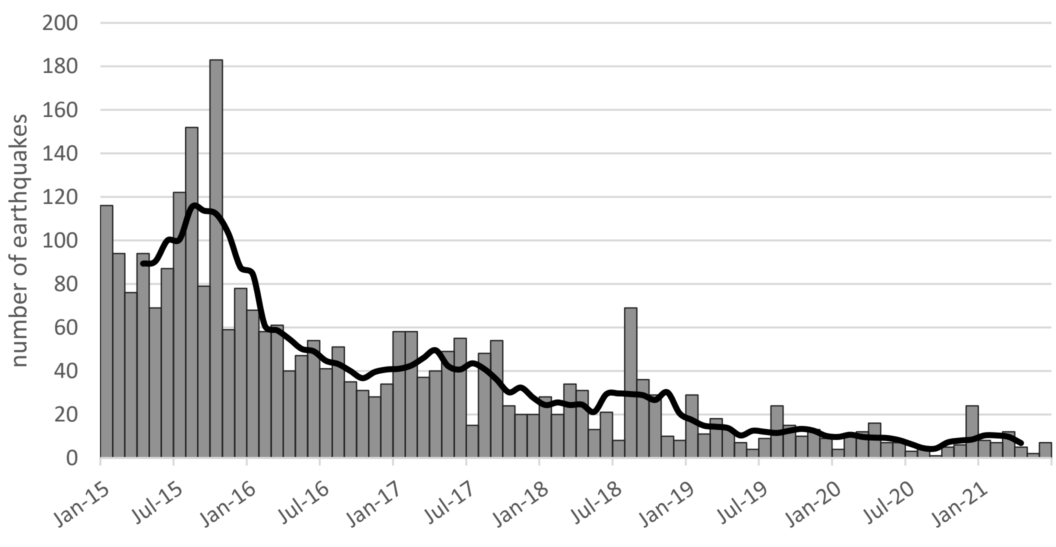

Figure 20. Monthly number of earthquakes M 2 or larger in south-central Kansas.

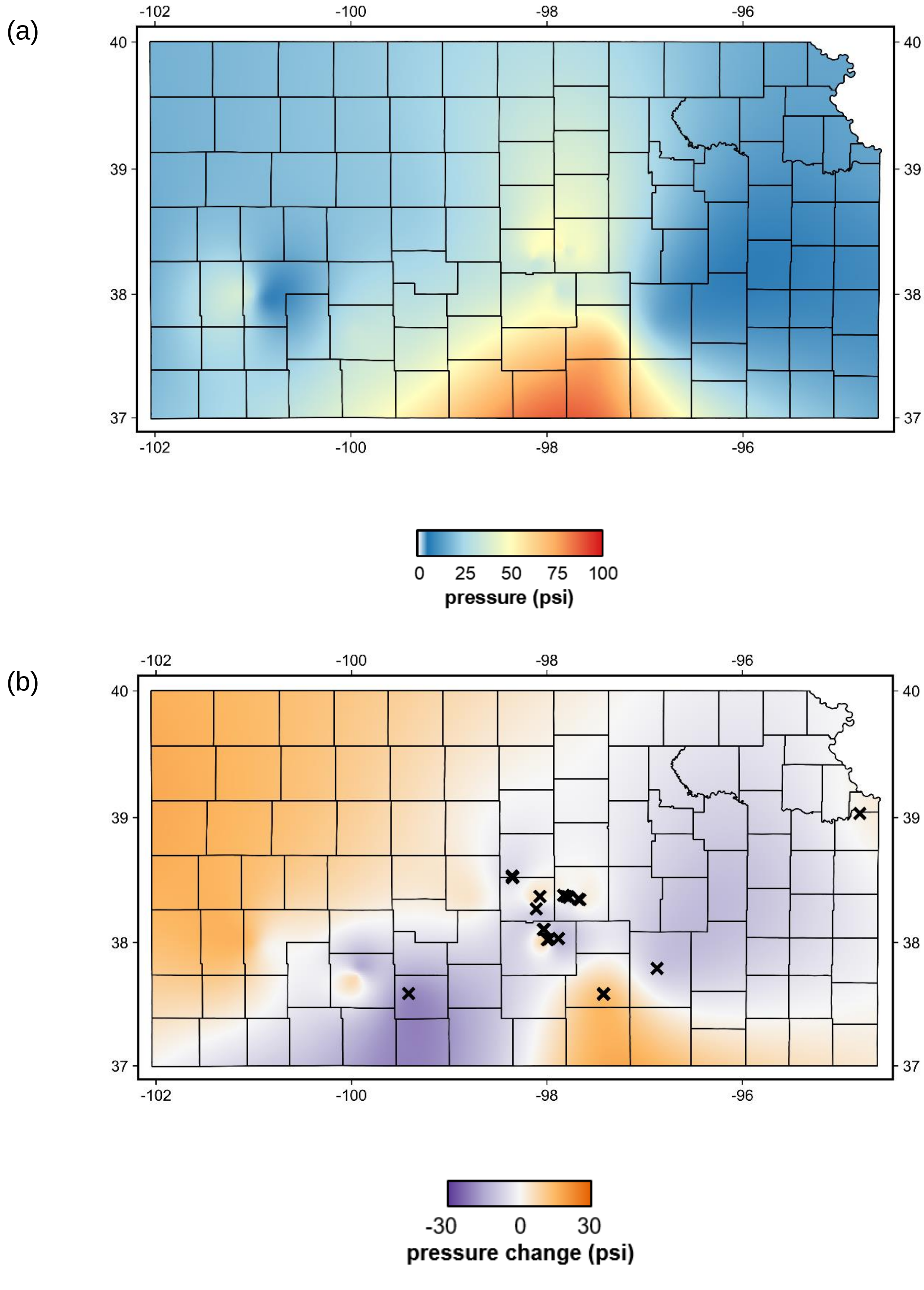

Figure 21. (a) Change in Arbuckle Group pore pressure in 2021 (relative to baseline pressures reported in 2002, or earliest available report thereafter). (b) Change in Arbuckle Group pore pressure from 2020 to 2022. Black Xs indicate Tier 1 member wells.

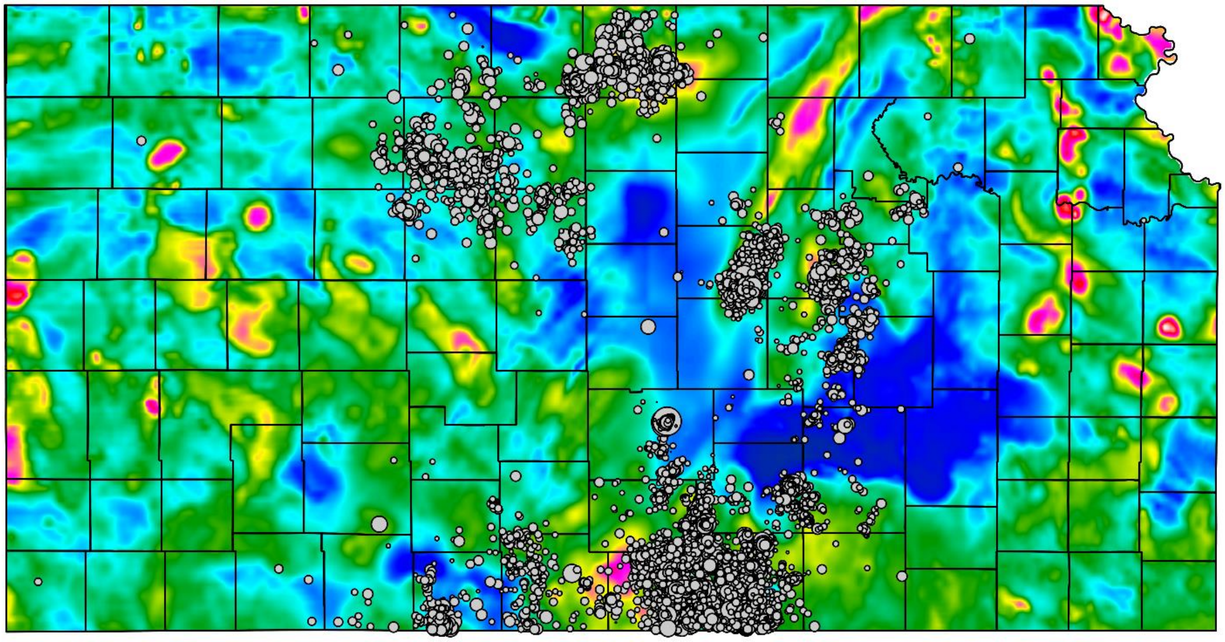

Figure 22. Earthquakes recorded by the KGS and CSTS networks from 2017-present superimposed on the aeromagnetic map of Kansas (Xia et al., 1995).

Integral to the magnetic susceptibility of rocks is their mineralogic and petrologic makeup and history. Basement rocks in Kansas have been identified from cored rock samples returned from boreholes that penetrated the Paleozoic section (Figure 23). An important caveat to comparison/correlations between basement rocks and magnetic susceptibility is the sampling depths of each. Basement rock types are identified from samples taken within the upper few to tens of feet of Precambrian rocks while the aeromagnetic values are from a much larger interval of rocks with significantly deep sampling depths. Therefore, correlations between seismicity (generally from epicenters around 3-4 miles deep) and basement rock types versus magnetic susceptibility need to consider the very uniquely different sampling characteristics of the material classifications. Key observations in both basement rock types and magnetic data are related to the gross/abrupt changes in measurements/material relative to boundaries of earthquake clustering/seismically active areas.

With the dramatic increase in seismicity from within Kansas basement rocks starting in 2013, coincident with the unprecedented increase in volume of fluid injected into the Arbuckle miles above the triggered faults, comes questions about fluid pathways from the Arbuckle into the basement rocks and then horizontal movement within the basement rocks. Important questions, and ones that could shed light on the reason for the occurrence of localized clusters of earthquakes in areas without large injection volumes or in some cases no injection, must consider localized and regional injected volumes along with the temporal progression of Arbuckle pressures and earthquakes from south-central Kansas into the central sections of the state (Peterie et al., 2020). An equally intriguing question relates to the trigger responsible for the series of earthquakes that started in 2013 in northcentral Kansas and moved from west to east, generally coincident with lineaments interpreted on magnetic susceptibility data (Figure 24). This overwhelming increase in subregional seismicity has no historical precedent.

Integration of seismicity, magnetic, and core data appears to suggest that a network of regional fluid pathways exists within basement rocks, with orientations consistent with lineaments on aeromagnetic data and somewhat controlled by boundaries between different basement rock types (Figure 25). These transport zones are likely controlled by fracture permeability and therefore allow pressure changes due the accumulation of fluids in the Arbuckle to drive relatively rapid changes in pore pressure in areas with critically stressed faults. Aseismic areas still likely contain these fluid passageways but don't have the critically stressed and properly oriented faults. Boundaries between critically stressed and properly oriented faults and faults without proper alignment with regional stress field have an unmistakable correlation with rock type/properties and major basement structures.

Saline County seismicity started in 2016 after more than 150 years of no reported or measured earthquakes. Since the current earthquake cluster began, the areal extent of the pattern has remained confined within a very localized (east and southeast portion of county) and well-defined polygon (Figure 26). This polygon overlays very closely the drill defined boundaries of the southern tip of the MGA and the truncation of spreading along the rift axis (Figure 27). The lack of localized injection volumes or changes in practice that would represent a potential mechanism for reaching and exceeding the triggering threshold, suggest pore pressure changes within this ancient tectonically active area likely are the result of cumulative and broad regional fluid loading in the Arbuckle.

Jewell County (as well as Smith, Osborne, Mitchell, and Republic) also host earthquakes that started in 2013 that have no historical precedent and are not consistent with any local (< 30 miles) injection activities. This surge in seismicity, coupled with both the aeromagnetic and

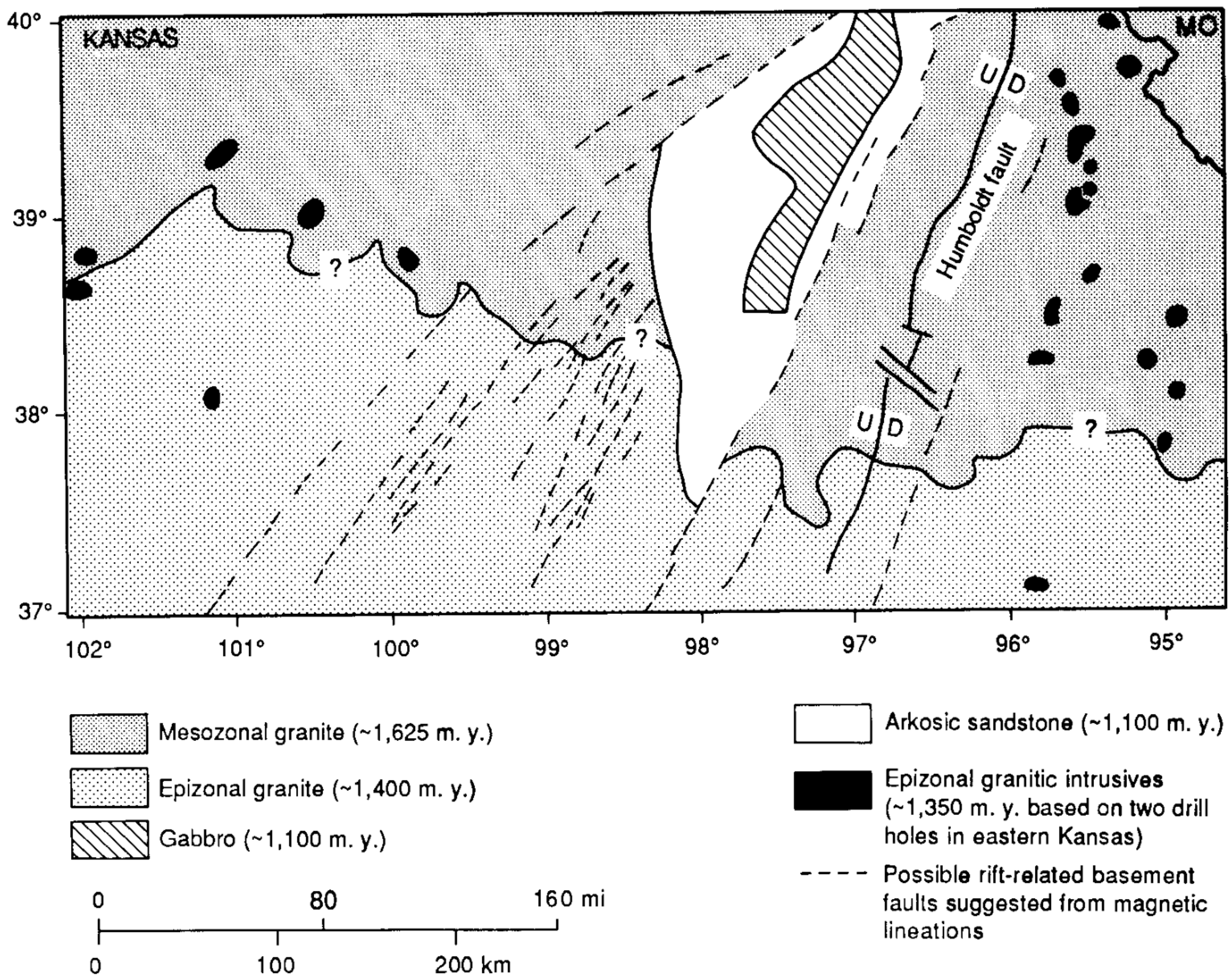

Figure 23. Precambrian terranes in Kansas. Interpreted from spectrally filtered magnetic maps and rock samples. From Yarger (1989).

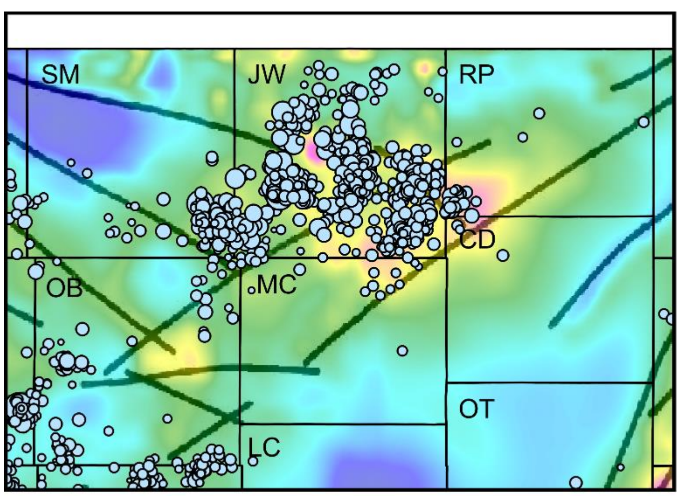

Figure 24. Earthquakes recorded by the KGS seismic network superimposed on the aeromagnetic map and interpreted magnetic lineaments (Yarger, 1983) in the Salina Basin.

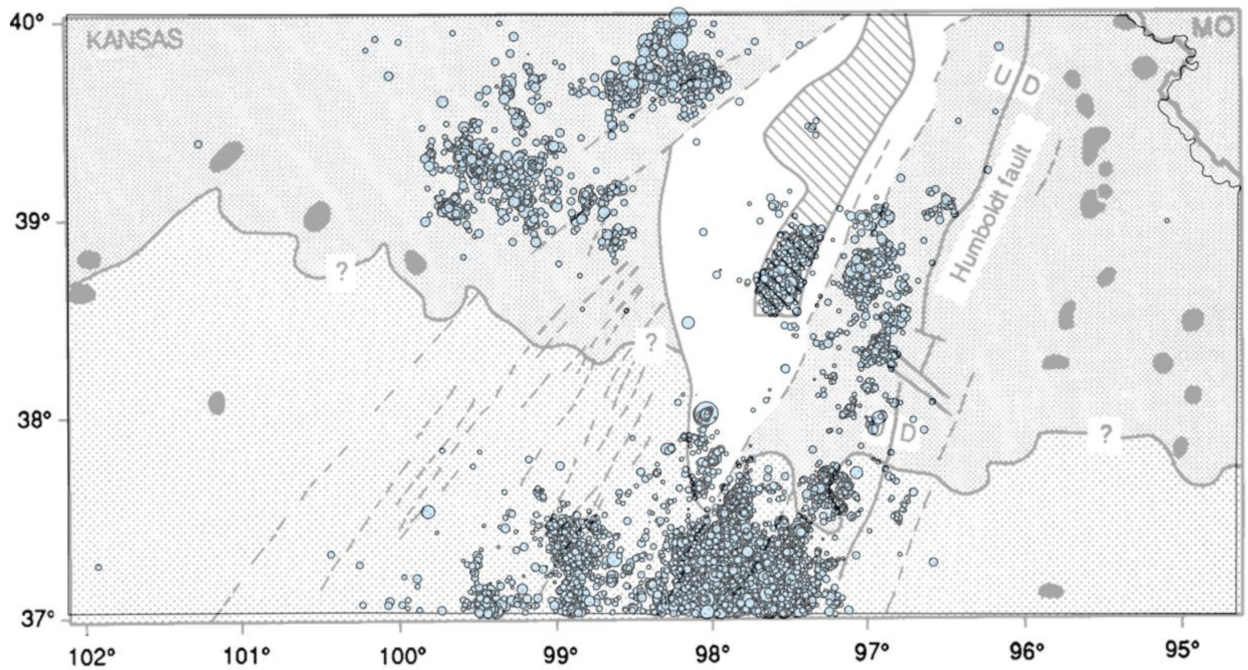

Figure 25. Earthquakes recorded by the KGS seismic network superimposed on the Precambrian terranes interpreted from magnetic maps and rock samples (see Figure 23 for interpreted rock types).

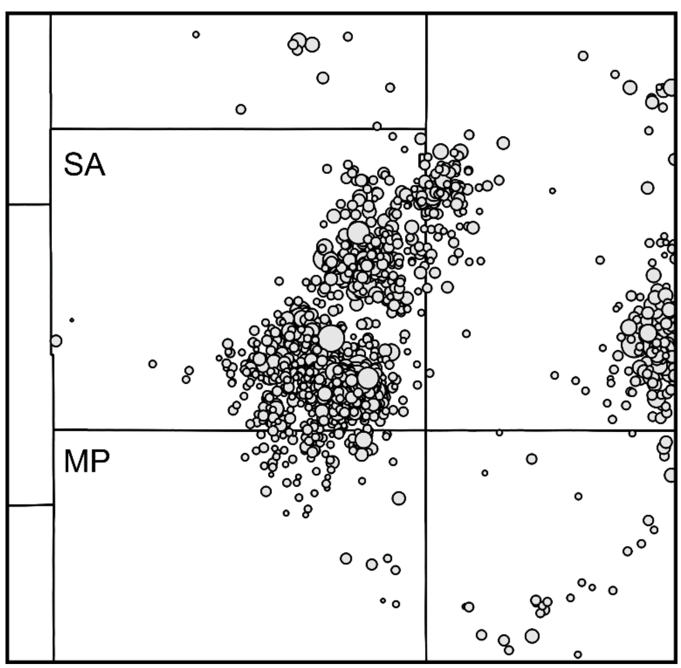

Figure 26. Earthquakes in the Saline County area recorded by the KGS seismic network from 2015 to present.

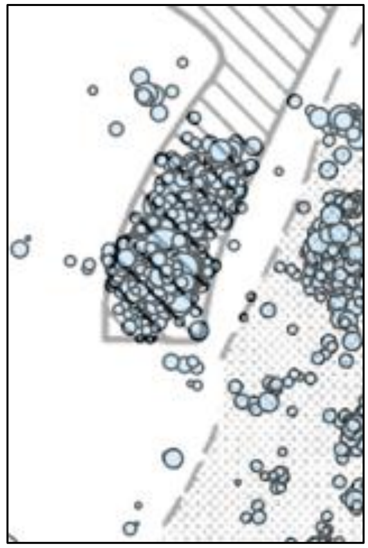

Figure 27. Earthquakes in the Saline County area recorded by the KGS seismic network from 2015 to present superimposed on the interpreted Precambiran terranes (see Figure 23).

basement rock map seems to suggest changes in Precambrian pore pressures along critically stressed and properly oriented faults could be a result of injection activities along a well-defined NE/SW trend (Figure 28). This trend appears to originate in NE Trego or SW Rooks County, with an aseismic area in central Osborne County. Southwestern Rooks County is characterized by a very significant linear NW/SE trend of earthquakes consistent with an aeromagnetic lineament. This correlation supports the suggestion that aeromagnetic data are providing evidence of faults, which are not properly aligned or are not critically stressed but represent zones of increased permeability and a transport pathway for fluid pressure changes.

A single earthquake that bears elevated attention is the M 2.9 event in Rice County. This event followed a marked one-year increase in subnetwork events with epicentral distances consistent with the location of the M 2.9. A primary driver for tracking subnetwork events is to help predict locations that are becoming seismically active and might be a catalyst for future felt events. Since this event is consistent in size with an earthquake recorded in 1981, this increase in subnetwork events and the eventual earthquake could be part of a natural sequence. However, Arbuckle pressures have been gradually increasing in Rice County and there is no way to predict the triggering threshold value. Continued monitoring of this particular epicentral distance will be critical to establishing if this is consistent with a 40-year event cycle or the start of a new cluster.

After more than a year since the swarm of felt events in the Hutchinson and Wichita areas it is possible to study the foreshock, mainshock, and aftershock sequence with the intent to search these data for patterns or indications as to their triggering sources. Based on the regional pressure history and the distribution of felt earthquakes, these two areas with significant clusters of earthquakes occurred over a fixed period of time, were well outside expectations of natural seismicity (according to historical records), and were likely due to a two-stage process. From all data currently available, it appears the triggering threshold was exceeded between 2012 and 2016 in these two areas and thereby brought the pore pressure on the faults to a ‘ready to slip’ level. From that point, injection practices (pulsing) at local wells previously tolerated by the nearby faults now instigate rupture for those critically stressed and properly aligned faults. This observation suggests that, in a pressure environment that exceeds the triggering threshold, until all

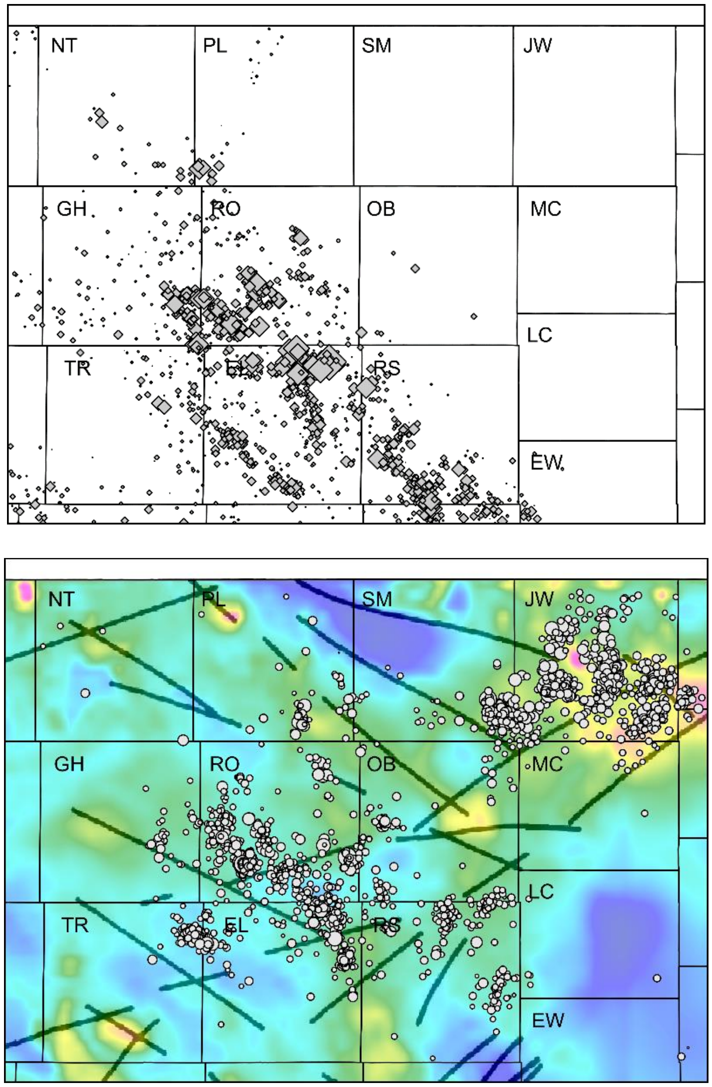

Figure 28. (a) Disposal wells and (b) earthquakes recorded by the KGS network from 2015 to present superimposed on the aeromagnetic map and interpreted magnetic lineaments (Yarger, 1983).

energy accumulated on critically stressed and properly aligned faults is dissipated through earthquakes, uniform and gradual injection volumes need to maintain historical average levels to avoid larger magnitude earthquakes.

Earthquakes occurring in related clusters will follow a statistical recursion relationship, which predicts the size and number of earthquakes over various periods of time based on the history and the Guttenberg-Richter relationship. In very general terms, that relationship designates that for each M 4 there will be 10 M 3s, 100 M 2s, and 1000 M 1s. It goes further to predict based on what is referred to as the b-index the time before various magnitude events in the future. It is therefore a very useful tool for predicting when to expect various size earth-quakes based on temporal and magnitude of previous earthquakes in a cluster.

Looking at each cluster as unique sequences of earthquake activity provides the best perspective for continued investigations into possible catalysts for the triggering of historically anomalous seismicity. For the Saline County cluster, predictions based on b-index have been extremely accurate over the last year. At the current rate and magnitude distribution a M 5 is statistically expected in 3 years. For Jewell County a M 5 is expected within 30 years. In Dickinson County a M 5 is due to occur within next 13 years at current rates and b-index. In Rooks County a M 5 should occur within 12 years. For the Hutchinson cluster we expect a M 5 within 8 years based on trends since 2015. For the Wichita cluster the calculation for the M 5 was made in June 2021 and a M 5 was expected within 1.4 years. However, based on the dramatic change in earthquake frequency and magnitudes we now estimate a M 5 should occur with 7.5 years.

WEB PAGE CONTENT

The CSTS web page (http://www.kgs.ku.edu/Geophysics/CSTS/index.html) is operated by the KGS. It includes links to information about meetings, publications, network updates, and seismic updates (for Tier 1 members) and information about the seismic network for Tier 2 members. It includes semi-annual newsletters about earthquake activity, along with access to a comprehensive catalog of events, including time, location, magnitude, and the Seismic Action Score (based on evaluation criteria developed by the State's Induced Seismicity Task Force) for each event. The website also includes a series of pictures and accounts of the installation process and gives a feel for the environment and footprint of each consortium station. Currently at least one station has been installed within 20 miles of every Tier 1 member's well (Figure 1, Appendix A). A short discussion and set of pictures are posted on the website documenting the installation process.

Beginning last year, the Publications section of the webpage includes a detailed overview of recent publications that may be relevant to Consortium members (https://www.kgs.ku.edu/Geophysics/CSTS/Group/recent_lit.html, Appendix D). For each paper, we provide three key points highlighting the primary findings and link to the full paper on the publisher's webpage. This section of the webpage will continue to be updated as new relevant papers are published. In time, we hope to provide detailed overviews for past induced seismicity publications as well. With the addition of MGP in Atchison the consortium network improves its sensitivity in the more populous northeastern portion of the state.

OTHER ACTIVITIES

The Consortium continued to meet remotely for both quarterly and annual meetings during the past reporting period. The annual meeting in August 2021 included a presentation by Dan Yates, now the executive director of the Groundwater Protection Council, which has long brought together regulators and researchers to discuss midcontinent induced seismicity and produced water issues. Those on-line reporting sessions were posted to the Consortium website. Plans were made for an in-person annual meeting (the first since 2019) to be held in August 2022.

PLANS

The Consortium continues to monitor pressures in the Arbuckle Formation and investigate the relationship between Arbuckle pressures, fluid levels, and seismicity. Dr. David Newell, recently retired from the KGS, has been retained to focus on Arbuckle measurements and issues. Consortium staff will also continue to investigate the relationship between geophysical anomalies and earthquake activity, as in Saline County, and analyze the recursion relationship between numerous smaller magnitude earthquakes and the possibility of larger magnitude events, particularly those in proximity to member facilities. Of particular interest will be the apparent correlations between basement geology and seismicity. Migration of seismicity around the state will also be a point of study.

CONCLUSION

The Consortium continues to monitor felt and micro-seismic activity with a high rate of station performance. The number of recorded earthquakes in south-central Kansas continued to drop, with less activity in the Reno and Sedgwick county area. However, the overall number of earthquakes that triggered alerts to Consortium members increased in the past reporting year, primarily due to a sharp increase in seismic activity in Saline County. A M 2.9 event in Rice County, an area with little historic record of activity, was also significant. The Consortium continues to monitor seismic activity and fluid injection practices with an eye toward identifying areas where micro-seismic activity may indicate a future increase in earthquakes, including the possibility of larger magnitude events.

REFERENCES

Armbruster, J.G., D.W. Steeples, and L. Seeber, 1989, The 1989 earthquake sequence near Palco, Kansas: A possible example of induced seismicity (abstract): *Seismological Research Letters*, v. 60, no. 4, p. 141.

Berendsen, P., and K.P. Blair, 1986, Subsurface structural maps over the central North American rift system (CNARS), central Kansas, with discussion: Kansas Geological Survey, Subsurface Geology Series 8, 16 p.

Buchanan, R., S. Peterie, R. Miller, 2021, Consortium to Study Trends in Seismicity, 2021 Annual report, 66 p.

Chan, C.-H., Y.-M. Wu, T.-L. Tseng, T.-L. Lin, and C.-C. Chen, 2012, Spatial and temporal evolution of b-values before large earthquakes in Taiwan: *Tectonophysics*, 532-535, 215-222.

Cole, V.B., 1976, Configuration of the top of the Precambrian rocks in Kansas: Kansas Geological Survey, Map M-7, scale 1:500,000.

El-Isa, Z.H., and D.W. Eaton, 2014, Spatiotemporal variations in the b-value of earthquake magnitude-frequency distributions: Classifications and causes: *Tectonophysics*, 615, 1-11.

Frohlich, C., and S.D. Davis, 1993, Teleseismic b Values; Or, Much Ado About 1.0: *Journal of Geophysical Research*, 98, 631-644

Geobel, T.H.W., S.M. Hosseini, F. Cappa, E. Hauksson, J.P. Ampuero, F. Aminzadeh, and J.B. Saleeby, 2016, Wastewater disposal and earthquake swarm activity at the southern end of the Central Valley, California: *Geophysical Research Letters*, 43, 1092-1099.

Haggenson, R., and H. Rajaram, 2021, Seismic diffusivity and the influence of heterogeneity on injection-induced seismicity: *Journal of Geophysical Research: Solid Earth*,126, e2021JB021768.

Healy, J.H., et al., 1968, The Denver Earthquakes: *Science*, v 161, no. 3848, p. 27.

Huang, Y., and G.C. Beroza, 2015, Temporal variation in the magnitude-frequency distribution during the Guy-Greenbrier earthquake sequence: *Geophysical Research Letters*, 42, 6639-6646.

Lay, T., and T.C. Wallace, 1995, Modern Global Seismology: Academic Press.

Wyss, M., and R. Stefansson, 2006, Nucleation Points of Recent Mainshocks in Southern Iceland, Mapped by b-Values: *Bulletin of the Seismological Society of America*, 96, 599-608.
Xia, J., R.D. Miller, and D.W. Steeples, 1995, Aeromagnetic map of Kansas, reduced to a horizontal plane and reduced to the pole: Kansas Geological Survey, Map Series M-41D.
Xia, J., R.D. Miller, D.W. Steeples, and D. Adkins-Heljeson, 1995, Residual Bouguer gravity map of Kansas, the second order regional trend removed: Kansas Geological Survey, Map Series M-41E.
Yarger, H.L., 1983, Regional interpretation of Kansas aeromagnetic data: Kansas Geological Survey, Geophysics Series 1, p. 1-35.
Yarger, H.L., 1989, Major magnetic features in Kansas and their possible geologic significance, in D. W. Steeples, ed., 1989, Geophysics in Kansas: Kansas Geological Survey, Bulletin 226, 197-213.
Zhai, G., M. Shirzaei, and M. Manga, 2020, Elevated Seismic Hazard in Kansas Due to High-Volume Injections in Oklahoma: *Geophysical Research Letters*, 47, e2019GL085705.

[This page is intentionally blank.]

Appendix A: CSTS Station Locations, Pictures, and Descriptions

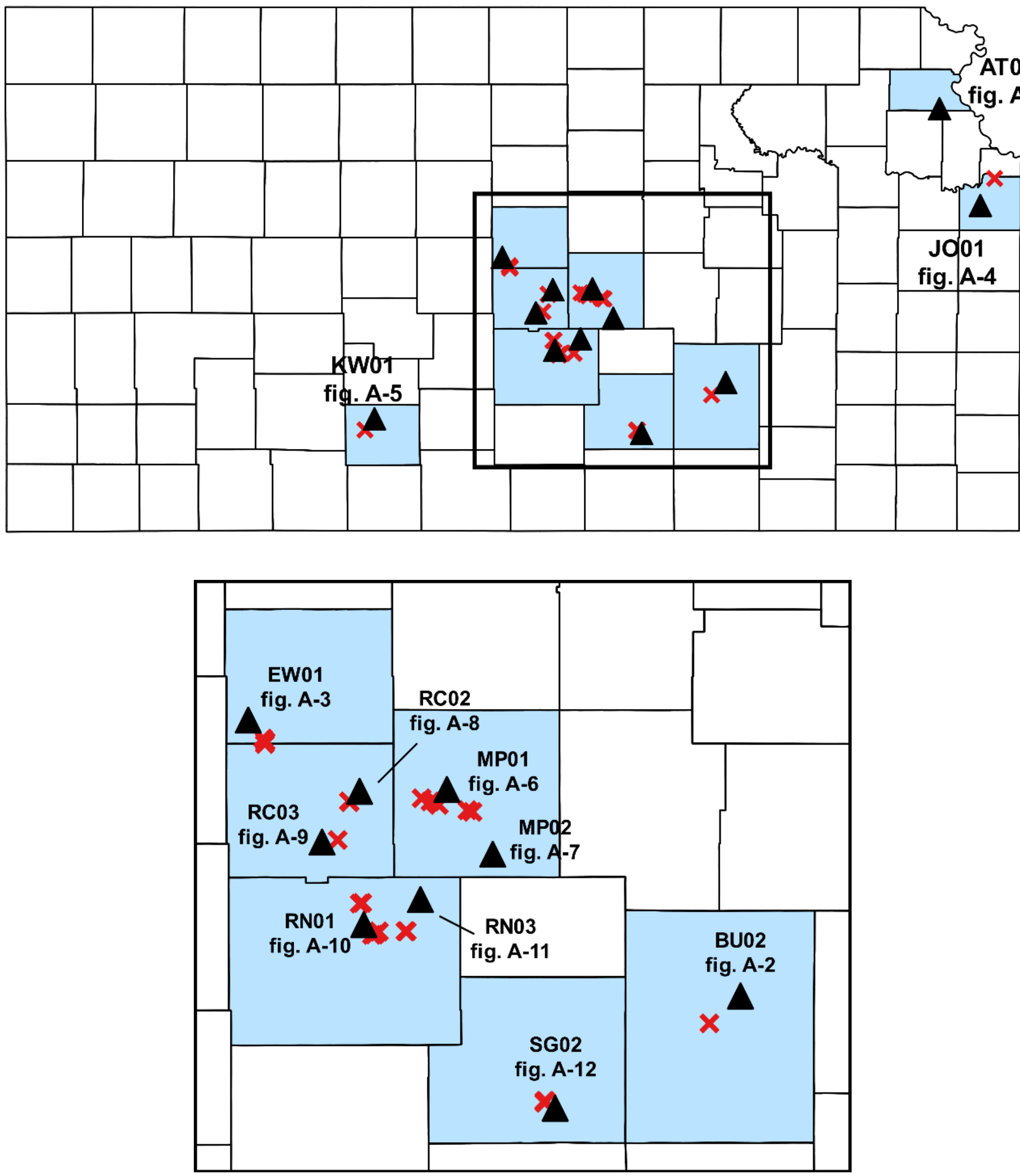

Figure A-0. Base map for pictures of equipment configuration at each station included in this appendix. Top figure is State of Kansas with the bottom figure enlargement of black box in upper figure. Black triangles are earthquake stations and red Xs are each member's injection facility location(s).

Figure A-2. AT01 is located in the Spring Hill Cemetery in southern Atchison County. This station is in a pasture near the El Dorado Lake about 2 mi from US Highway 59.

Figure A-2. BU02 is located in the El Dorado State Park in northern Butler County. This station is in a pasture near the El Dorado Lake about 4 mi from Interstate 35.

Figure A-3. EW01 is located in southwestern Ellsworth County near the city of Holyrood. The station is in a cemetery about 1 mi from highway Kansas Highway 156.

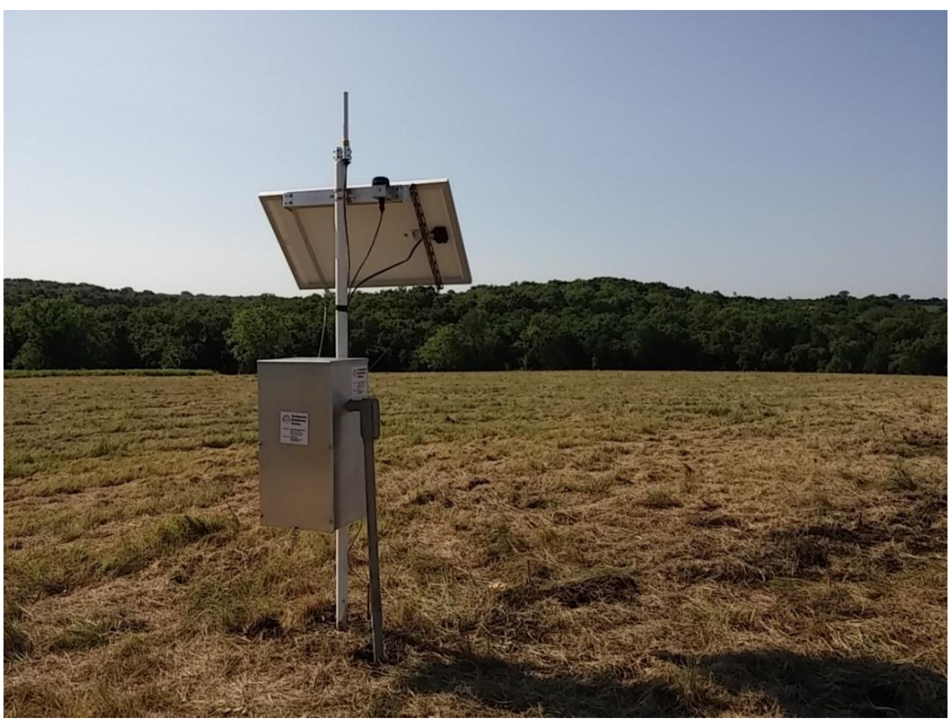

Figure A-4. JO01 is located on the grounds of the Olathe Prairie Center in Johnson County about 4 mi west of Kansas Highway 10. There is light traffic around the station and two rock quarries within about 5 mi.

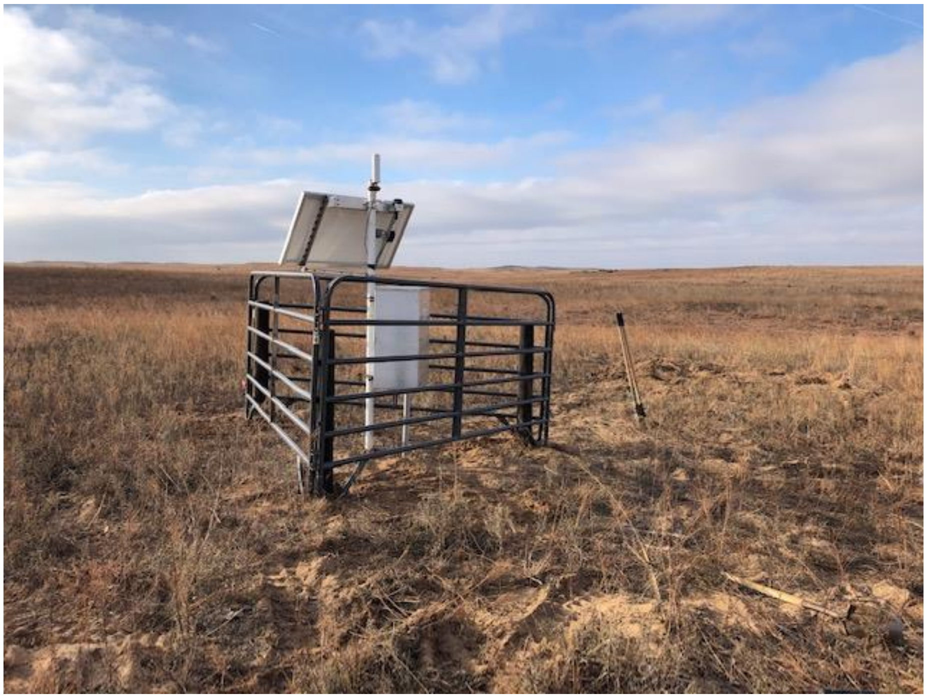

Figure A-5. KW02 is located in northern Kiowa County in a pasture located between Mullinville and Greensburg more than 1 mi from the railroad and highway.

Figure A-6. MP01 is located in the McPherson Valley Wetlands Wildlife Area in McPherson County. The station is northwest of Conway about 2 mi from US Highway 56.

Figure A-7. MP02 is located in south-central McPherson County about 10 miles south of McPherson. The station is in a pasture on the grounds of a local church about 3 mi from Interstate 135.

Figure A-8. RC02 is located in eastern Rice County near the city of Little River. This station is installed in a pasture more than 1 mi from US Highway 56 and Kansas Highway 46.

Figure A-9. RC03 is located in Rice County between Lyons and Sterling. This station is installed in a pasture about 2 mi from Kansas Highway 96 and is near a small landing strip.

Figure A-10. RN01 is located in Reno County west of Hutchison. This station is installed in a cemetery about 2 mi from Kansas Highway 14.

Figure A-11. RN03 is located in Reno County northeast of Hutchison in Sand Hills State Park. It is installed about 2.5 mi from Kansas Highway 61.

Figure A-12. SG02 is located in Sedgwick County south of Wichita. This station is on the grounds of a local church about 3 mi from Interstate 35 and US Highway 81 and 2 mi from two sets of railroad tracks to the west and east.

[This page is intentionally blank.]

Appendix B: CSTS Earthquake Catalog

This catalog includes all earthquakes that were uniquely located and within 20 miles of a consortium member facility from July 1, 2021, to June 30, 2022.

Origin Time (UTC)	Latitude	Longitude	Magnitude
2021-07-02 05:33:10	37.69337	-97.23030	0.8
2021-07-05 09:47:03	38.51104	-97.55045	1.1
2021-07-05 11:33:18	37.67733	-97.22327	1.4
2021-07-05 12:06:19	37.69272	-97.24539	2.1
2021-07-05 12:31:28	37.67878	-97.21407	1.2
2021-07-05 12:46:16	37.67106	-97.22270	1.1
2021-07-05 13:31:59	37.69020	-97.21140	2.0
2021-07-06 17:28:15	37.60486	-97.21828	1.3
2021-07-07 11:11:56	37.69316	-97.24141	1.6
2021-07-07 11:19:43	37.70041	-97.23245	1.6
2021-07-08 22:26:46	37.54749	-97.77132	1.3
2021-07-09 09:21:30	37.59733	-97.24688	1.7
2021-07-10 08:34:11	38.57876	-97.59389	1.4
2021-07-11 08:24:30	37.69378	-97.19048	1.3
2021-07-11 09:20:46	37.49308	-97.73569	1.1
2021-07-11 09:45:15	37.50839	-97.71996	1.1
2021-07-13 17:25:57	37.51769	-97.72227	1.1
2021-07-13 20:16:16	37.62878	-97.74416	1.7
2021-07-13 21:53:17	37.63590	-97.73168	1.7
2021-07-14 11:56:55	38.01371	-97.99110	1.3
2021-07-14 13:40:10	37.70901	-97.23161	1.7
2021-07-17 02:43:10	38.01585	-97.98830	2.6
2021-07-17 03:06:06	38.01985	-97.99049	2.4
2021-07-17 08:12:19	38.01519	-97.99129	2.7
2021-07-17 09:10:14	38.01771	-97.99103	1.4
2021-07-17 09:19:23	38.01864	-97.98929	1.5
2021-07-19 21:07:58	37.69604	-97.22729	1.8
2021-07-21 07:47:57	38.01958	-97.98040	1.4
2021-07-22 13:13:12	37.65436	-97.73204	1.2
2021-07-27 03:35:17	37.70039	-97.21740	1.5
2021-07-28 23:09:11	37.29949	-97.41491	1.2
2021-07-28 23:25:35	37.30534	-97.40660	1.5
2021-07-29 10:01:43	37.29560	-97.42136	1.7
2021-07-29 19:57:37	37.30525	-97.39922	1.5
2021-08-04 03:38:09	37.60495	-97.24426	0.8
2021-08-04 03:39:10	37.57005	-97.27816	0.6
2021-08-05 18:28:13	37.65158	-97.56013	2.1
2021-08-05 19:21:02	37.61969	-97.56402	1.1
2021-08-07 13:51:20	37.63143	-97.74312	1.7
2021-08-09 07:17:37	37.70778	-97.21909	1.4
2021-08-10 03:25:08	37.64153	-97.74110	1.9
2021-08-12 12:37:29	37.64056	-97.73198	2.4
2021-08-17 10:41:02	38.58564	-97.62379	1.4
2021-08-20 01:11:36	38.01627	-97.98643	1.4
2021-08-21 02:00:40	37.29395	-97.42508	1.5
2021-08-31 22:13:24	37.43384	-97.68549	1.5
2021-09-08 19:56:03	37.60831	-97.74615	1.5
2021-09-10 04:08:18	37.68371	-97.21803	1.8
2021-09-10 04:09:23	37.69685	-97.25652	1.5
2021-09-10 05:04:56	37.68718	-97.23016	1.3
2021-09-10 05:57:27	37.68227	-97.21068	1.3
2021-09-10 09:30:46	37.69190	-97.20728	1.3
2021-09-19 07:52:46	37.69090	-97.22810	1.3
2021-09-19 08:33:28	37.70124	-97.23509	1.7
2021-09-19 10:31:06	37.32364	-97.39422	1.1
2021-09-26 21:07:22	37.68303	-97.19559	1.5
2021-10-03 00:29:27	38.53630	-97.53738	1.3
2021-10-05 03:31:20	38.58836	-97.59618	1.2
2021-10-22 08:47:03	38.53844	-97.60929	1.8

Origin Time (UTC)	Latitude	Longitude	Magnitude
2021-10-24 22:33:11	37.63918	-97.26352	2.5
2021-11-11 23:31:15	37.68923	-97.21251	1.3
2021-11-20 12:22:29	38.24260	-97.48433	2.2
2021-11-21 18:34:57	37.76519	-97.99465	1.7
2021-11-30 23:11:42	37.76858	-97.08285	1.5
2021-12-02 11:10:14	38.02377	-97.07900	1.2
2021-12-11 00:01:59	38.61332	-97.53800	1.6
2021-12-11 00:12:28	38.60049	-97.52444	1.5
2021-12-15 23:12:13	38.58393	-97.54043	1.9
2021-12-29 17:49:14	38.58189	-97.52106	1.3
2021-12-29 18:03:57	38.54839	-97.56369	1.3
2021-12-30 03:10:14	37.86610	-98.02665	1.4
2022-01-03 07:06:14	37.59062	-97.50199	1.6
2022-01-03 07:26:00	37.45643	-97.68958	1.1
2022-01-06 02:35:37	37.42281	-97.68512	1.6
2022-01-07 11:46:02	38.60149	-97.53030	1.4
2022-01-07 16:59:59	37.63675	-97.29714	1.8
2022-01-10 05:32:20	38.40456	-97.31403	1.1
2022-01-11 14:56:05	38.60142	-97.53572	1.5
2022-01-12 21:44:13	37.65745	-97.09322	1.5
2022-01-13 05:23:39	38.60400	-97.51157	1.0
2022-01-24 00:13:45	38.57804	-97.64039	1.4
2022-01-27 11:42:07	37.67098	-97.20924	1.5
2022-02-06 06:00:18	37.64337	-97.33491	1.1
2022-02-19 21:53:18	37.44321	-97.67028	1.9
2022-02-20 07:08:46	37.70747	-97.23845	1.9
2022-02-20 07:35:13	37.77013	-97.26775	1.4
2022-02-20 07:44:03	37.67890	-97.22530	1.7
2022-02-24 05:49:07	38.61661	-97.63261	1.6
2022-02-24 19:06:46	37.59180	-96.80764	1.4
2022-02-27 10:36:18	37.54060	-97.77580	1.4
2022-02-28 07:50:43	37.88145	-98.07227	1.4
2022-02-28 08:39:13	37.88696	-98.09802	1.2
2022-03-09 07:49:50	38.62801	-97.62121	1.4
2022-03-11 17:41:21	38.61996	-97.59682	2.0
2022-03-12 16:23:40	38.61781	-97.59827	2.2
2022-03-14 01:15:02	38.62141	-97.58345	1.6
2022-03-17 02:27:00	38.62399	-97.59811	1.9
2022-03-17 20:42:09	37.31672	-97.45345	2.0
2022-03-18 01:12:29	37.31520	-97.47582	2.0
2022-03-19 01:03:58	37.51945	-97.75692	2.2
2022-03-19 04:26:09	37.51724	-97.75138	2.7
2022-03-19 04:27:14	37.51640	-97.75407	3.4
2022-03-19 04:46:53	37.51365	-97.75434	1.6
2022-03-19 04:50:51	37.52549	-97.75051	2.0
2022-03-19 05:25:50	37.54625	-97.74445	1.7
2022-03-19 06:49:11	37.51970	-97.74036	1.3
2022-03-19 12:26:21	37.51190	-97.74860	2.8
2022-03-20 00:00:14	37.52091	-97.74859	3.7
2022-03-20 00:05:18	37.52494	-97.76167	2.9
2022-03-20 00:10:08	37.54595	-97.76122	1.7
2022-03-20 00:32:26	37.52775	-97.72962	1.5
2022-03-20 01:08:08	37.52132	-97.74063	1.4
2022-03-20 01:22:28	37.52774	-97.72823	1.6
2022-03-20 02:15:52	37.51015	-97.75833	1.5
2022-03-20 02:40:43	37.50600	-97.74200	1.7
2022-03-20 02:43:33	37.51644	-97.74801	2.5
2022-03-20 03:08:08	37.55575	-97.70163	1.2
2022-03-20 05:39:45	37.52730	-97.73869	1.2

Appendix B. Continued

Origin Time (UTC)	Latitude	Longitude	Magnitude
2022-03-20 06:16:45	37.51150	-97.74828	1.3
2022-03-20 08:31:16	37.50939	-97.75018	2.3
2022-03-20 08:51:00	37.51348	-97.74706	2.8
2022-03-20 15:40:32	37.51265	-97.74914	2.6
2022-03-22 00:33:22	37.51019	-97.75558	3.1
2022-03-22 01:49:00	37.51722	-97.74292	1.6
2022-03-22 03:11:30	37.51542	-97.74589	1.4
2022-03-22 04:43:12	37.52918	-97.75571	1.1
2022-03-22 06:13:16	37.51513	-97.74519	2.1
2022-03-22 10:51:03	38.62128	-97.58324	1.7
2022-03-22 16:20:55	37.51237	-97.74071	2.1
2022-03-23 08:27:03	38.62637	-97.61318	1.9
2022-03-24 08:10:09	38.61600	-97.59779	1.1
2022-03-24 15:33:58	37.52990	-97.75826	1.6
2022-03-24 15:50:24	37.51276	-97.75396	1.9
2022-03-25 08:17:22	37.51352	-97.76853	1.3
2022-03-25 16:22:30	37.51858	-97.74971	1.4
2022-03-26 02:13:03	37.51025	-97.73382	1.5
2022-03-27 04:47:12	37.51455	-97.74386	2.4
2022-03-28 10:34:20	38.98312	-95.06104	1.3
2022-03-28 12:41:36	38.61472	-97.58698	2.0
2022-03-31 03:29:00	37.52200	-97.74395	1.5
2022-04-04 07:29:52	38.53116	-97.56034	1.4
2022-04-05 06:41:34	38.00043	-96.97284	0.8
2022-04-05 10:20:22	38.60873	-97.59891	1.8
2022-04-07 12:02:32	38.60996	-97.54771	1.8
2022-04-07 12:08:25	37.45300	-97.67351	1.5
2022-04-09 16:32:40	38.62316	-97.57350	1.9
2022-04-17 10:09:53	37.89572	-98.06088	1.6
2022-05-03 10:26:46	37.63700	-97.74000	1.5
2022-05-04 01:38:32	37.53901	-97.71294	1.5
2022-05-14 07:32:42	38.61970	-97.59143	1.2
2022-05-17 02:23:50	38.01310	-97.98891	2.6
2022-05-17 05:58:29	37.51574	-97.74685	1.8
2022-05-18 14:41:56	38.00887	-97.98232	1.7
2022-05-18 14:45:43	38.02226	-97.98154	1.3
2022-06-09 23:29:29	37.99789	-97.05057	1.4
2022-06-20 04:35:50	37.71091	-97.23098	1.2
2022-06-28 22:24:01	38.47393	-98.10242	2.9

End of table

Appendix C: Subnetwork Events Catalog

Subnetwork events recorded from July 1, 2021, to June 30, 2022, with epicentral distance within 12 miles of member wells. Epicentral distance is the estimated distance from the earthquake epicenter to the seismic station where it was recorded.

Station	Origin Time (UTC)	Distance (mi)	Magnitude
AT01	2022-01-17 17:27:22	0.3	-1.5
AT01	2022-02-23 02:58:54	5.0	-0.4
AT01	2022-05-01 14:49:09	1.3	-1.5
BU02	2021-07-01 07:45:26	2.2	-0.6
BU02	2021-07-04 21:00:07	7.4	0.2
BU02	2021-09-15 03:30:33	4.0	0.7
BU02	2021-09-29 23:43:11	11.4	0.1
BU02	2021-10-11 01:20:39	9.1	-0.2
BU02	2022-01-02 03:20:05	0.8	-1.5
BU02	2022-01-02 04:48:49	1.0	-1.5
BU02	2022-01-02 06:02:29	1.0	-1.5
BU02	2022-01-02 06:12:39	1.6	-1.5
BU02	2022-01-02 08:28:13	1.7	-0.9
BU02	2022-01-02 09:25:57	0.4	-1.5
BU02	2022-01-02 12:12:13	0.5	-1.5
BU02	2022-01-02 12:31:29	0.6	-1.5
BU02	2022-01-02 12:39:20	0.9	-1.5
BU02	2022-01-02 12:39:59	1.2	-1.5
BU02	2022-01-02 12:50:55	0.8	-0.9
BU02	2022-01-02 13:49:37	2.3	-1.5
BU02	2022-01-02 14:00:42	1.1	-1.5
BU02	2022-01-10 07:50:31	2.0	-0.9
BU02	2022-01-20 12:27:14	1.2	-1.5
BU02	2022-01-21 03:43:48	0.7	-1.5
BU02	2022-01-21 04:55:22	1.4	-1.5
BU02	2022-02-04 16:05:45	0.8	-0.9
BU02	2022-02-05 03:06:19	2.3	-0.9
BU02	2022-02-19 16:50:59	1.7	-1.5
BU02	2022-02-23 06:24:05	1.3	-1.5
BU02	2022-02-23 07:54:12	1.5	-1.5
BU02	2022-02-23 07:59:08	2.2	-0.9
BU02	2022-02-23 08:46:12	1.5	-1.5
BU02	2022-02-23 08:48:47	1.1	-1.5
BU02	2022-02-23 08:50:03	1.4	-1.5
BU02	2022-02-23 09:28:40	1.3	-1.5
BU02	2022-02-23 10:13:43	1.1	-1.5
BU02	2022-02-23 11:02:22	0.9	-1.5
BU02	2022-02-23 11:08:01	1.5	-1.5
BU02	2022-02-23 12:07:36	0.9	-1.5
BU02	2022-02-23 12:12:34	1.2	-1.5
BU02	2022-02-23 12:14:56	1.2	-1.5
BU02	2022-02-23 12:17:01	0.5	-1.5
BU02	2022-02-23 12:17:08	0.8	-1.5
BU02	2022-04-30 01:37:59	3.4	0.0
EW01	2021-07-01 23:47:23	6.6	0.1
EW01	2021-07-07 01:17:12	1.8	-0.9
EW01	2021-09-02 05:03:12	7.4	0.0
EW01	2021-09-16 05:48:37	1.9	-0.4
EW01	2021-09-16 06:09:58	3.5	-0.2
EW01	2021-09-27 21:36:54	1.7	-0.9
EW01	2021-09-28 16:12:08	1.8	-0.9
EW01	2021-09-30 08:10:26	3.2	-0.2
EW01	2021-10-13 05:51:53	4.8	-0.2
EW01	2022-03-27 03:07:24	11.8	0.5
EW01	2022-04-06 04:44:15	4.1	0.3
EW01	2022-05-22 19:00:41	1.6	-0.4
EW01	2022-06-05 08:02:16	11.3	1.5
JO01	2021-12-19 05:47:37	1.1	-0.2
JO01	2022-01-07 14:39:38	2.3	-0.6
JO01	2022-01-21 10:07:47	1.1	-1.5
JO01	2022-03-08 06:28:37	2.4	-1.5
JO01	2022-03-23 10:04:06	2.1	-0.9
JO01	2022-03-28 10:34:24	10.8	0.1
JO01	2022-05-24 16:04:27	10.4	0.4
KW02	2021-07-03 20:16:40	4.7	-0.2
KW02	2021-08-29 10:35:21	3.7	-0.4
KW02	2021-09-30 10:05:33	2.3	-0.2
KW02	2021-12-29 05:15:58	2.1	-0.9
KW02	2022-01-19 02:08:52	1.2	-1.5
KW02	2022-02-01 05:54:20	3.4	-1.5
KW02	2022-02-19 02:47:10	2.0	-0.9
KW02	2022-04-04 03:37:26	1.0	-0.9
KW02	2022-04-04 09:36:54	4.9	0.1
KW02	2022-04-09 09:07:33	1.0	-0.9
KW02	2022-04-11 10:46:30	2.5	-0.6
KW02	2022-04-24 10:01:34	3.9	0.0
KW02	2022-04-24 10:13:15	4.4	0.0
KW02	2022-04-26 09:42:21	4.5	0.1
KW02	2022-05-17 04:25:48	0.7	-1.5
KW02	2022-05-23 01:17:32	1.9	-0.6
KW02	2022-06-01 02:56:03	2.3	-0.6
MP01	2021-07-02 14:04:11	0.9	-1.5
MP01	2021-07-02 14:04:11	1.2	-1.5
MP01	2021-07-03 06:27:04	1.5	-0.9
MP01	2021-09-07 01:12:28	2.4	-0.9
MP01	2021-09-08 13:15:08	4.3	-0.6
MP01	2021-09-08 20:11:30	1.2	-0.4
MP01	2021-09-14 00:59:21	1.5	-0.9
MP01	2021-09-17 23:07:04	2.7	-0.9
MP01	2021-09-22 07:24:19	6.0	-0.6
MP01	2021-09-23 11:07:15	1.9	-0.6
MP01	2021-09-23 11:07:15	1.8	-0.9
MP01	2021-10-09 01:16:30	3.5	-0.6
MP01	2021-10-21 08:51:54	5.9	-0.2
MP01	2021-11-04 12:22:39	4.7	0.3
MP01	2021-11-06 12:12:37	2.4	-0.2
MP01	2021-11-06 12:13:58	11.6	0.5
MP01	2021-11-20 10:53:21	3.6	-0.4
MP01	2021-11-24 09:19:58	9.4	0.0
MP01	2021-11-29 07:16:18	4.4	0.1
MP01	2021-12-02 20:41:19	1.5	0.1
MP01	2021-12-12 06:28:46	1.1	-0.9
MP01	2021-12-24 06:09:57	1.0	-0.9
MP01	2021-12-27 02:27:20	6.6	0.6
MP01	2022-01-03 00:15:58	3.4	0.4
MP01	2022-01-10 02:12:11	2.1	0.0
MP01	2022-01-11 06:08:40	0.8	-1.5
MP01	2022-01-11 06:24:19	3.9	-0.6
MP01	2022-01-12 10:18:20	1.8	-0.9
MP01	2022-02-10 09:51:54	2.3	0.0

Appendix C. Continued

Station	Origin Time (UTC)	Distance (mi)	Magnitude
MP01	2022-02-15 04:06:55	1.2	-1.5
MP01	2022-02-19 03:58:04	2.8	-0.9
MP01	2022-02-20 07:17:24	5.7	-0.6
MP01	2022-02-20 07:36:33	8.0	0.1
MP01	2022-05-04 22:37:44	2.4	-0.6
MP01	2022-05-06 10:13:31	7.0	0.1
MP01	2022-05-08 23:57:57	1.4	-0.9
MP01	2022-05-10 22:35:08	1.5	-0.6
MP01	2022-05-14 02:00:50	4.5	-0.2
MP01	2022-05-17 02:27:51	4.3	0.1
MP01	2022-05-22 13:37:13	2.2	-0.9
MP01	2022-06-05 07:08:15	4.8	0.4
MP01	2022-06-08 08:35:11	6.0	0.2
MP02	2021-07-05 05:12:19	3.8	-0.6
MP02	2021-07-05 20:23:00	3.0	-0.9
MP02	2021-08-20 04:28:52	3.6	-0.6
MP02	2021-08-25 10:44:08	1.4	-1.5
MP02	2021-09-11 12:36:05	3.4	-0.6
MP02	2021-09-11 12:44:59	6.8	-0.2
MP02	2021-09-11 15:29:36	1.0	-1.5
MP02	2021-09-13 07:04:16	7.0	-0.4
MP02	2021-09-17 07:01:49	6.6	-0.2
MP02	2021-09-23 05:33:42	4.1	-0.9
MP02	2021-09-23 07:11:23	2.1	-0.9
MP02	2021-09-29 05:53:04	2.7	-0.6
MP02	2021-10-08 08:57:18	1.6	-0.6
MP02	2021-10-13 23:56:35	1.9	-1.5
MP02	2021-11-07 13:56:29	5.6	-0.2
MP02	2021-11-10 16:29:20	3.1	-0.6
MP02	2021-11-20 10:12:39	7.0	-0.2
MP02	2021-12-15 02:59:05	5.4	0.0
MP02	2021-12-19 01:57:15	5.7	-0.2
MP02	2021-12-25 12:17:04	2.4	-0.9
MP02	2021-12-26 22:22:18	3.0	-0.9
MP02	2022-01-03 10:35:03	0.7	-1.5
MP02	2022-01-03 20:05:34	1.5	-1.5
MP02	2022-02-10 02:18:21	1.6	-0.9
MP02	2022-02-10 02:18:21	1.7	-0.6
MP02	2022-02-10 02:18:21	1.4	-0.9
MP02	2022-02-18 04:46:25	1.0	-1.5
MP02	2022-02-19 10:51:44	3.9	-0.2
MP02	2022-04-09 14:24:17	0.5	-0.6
MP02	2022-04-11 18:17:47	1.4	-0.6
MP02	2022-04-20 23:50:30	4.2	-0.9
MP02	2022-04-25 05:20:01	1.6	-0.4
MP02	2022-05-01 06:54:01	0.3	-1.5
MP02	2022-05-20 02:51:49	2.7	-0.6
MP02	2022-05-23 04:54:03	3.2	0.0
MP02	2022-05-27 09:22:55	7.0	0.4
MP02	2022-06-14 07:13:28	4.4	0.2
RC02	2021-07-02 00:04:38	4.1	-0.6
RC02	2021-07-02 03:34:42	0.6	-1.5
RC02	2021-07-08 07:12:26	4.7	-0.6
RC02	2021-08-26 04:16:11	5.1	-0.6
RC02	2021-08-26 04:31:52	6.8	-0.6
RC02	2021-09-05 01:42:20	0.4	-0.9
RC02	2021-09-05 01:45:13	0.6	-0.6
RC02	2021-09-15 02:51:31	2.7	-0.9
RC02	2021-09-15 04:00:41	1.3	-0.6
RC02	2021-09-24 00:46:04	2.1	-0.2
RC02	2021-09-29 02:00:30	2.7	0.1
RC02	2021-09-29 05:07:37	1.4	-0.9
RC02	2021-10-02 07:12:35	0.9	-0.9
RC02	2021-10-05 00:49:57	3.6	-0.4
RC02	2021-10-12 04:51:51	1.5	-0.9
RC02	2021-11-16 14:48:44	11.6	1.1
RC02	2021-12-16 07:54:30	1.8	-0.6
RC02	2021-12-16 14:53:50	1.8	0.0
RC02	2022-01-02 14:15:19	8.3	-0.6
RC02	2022-02-24 06:43:39	2.0	-0.4
RC02	2022-03-06 19:29:55	5.6	0.4
RC02	2022-05-02 21:51:07	3.0	0.0
RC02	2022-05-17 12:38:37	1.2	-0.9
RC02	2022-05-18 04:25:10	6.2	-0.2
RC02	2022-05-31 06:45:24	3.1	-0.2
RC02	2022-06-01 18:29:19	8.0	0.3
RC03	2021-08-13 03:34:28	1.4	-0.9
RC03	2021-09-13 18:27:07	6.7	-0.4
RC03	2021-09-17 22:36:58	2.0	-0.9
RC03	2021-09-21 18:18:30	6.7	0.0
RC03	2021-09-28 20:13:11	3.1	-0.9
RC03	2021-10-01 06:35:34	6.8	0.1
RC03	2021-10-13 10:08:27	7.2	0.2
RC03	2021-12-02 20:53:28	7.1	-0.4
RC03	2022-01-20 23:48:49	1.4	-0.9
RC03	2022-01-21 07:21:55	2.0	-1.5
RC03	2022-02-06 04:06:14	3.7	-0.6
RC03	2022-02-21 05:33:53	7.6	0.0
RC03	2022-04-26 22:09:47	6.7	0.6
RC03	2022-05-18 04:56:37	1.0	0.0
RC03	2022-05-20 22:56:24	7.0	0.1
RN01	2021-07-02 03:36:14	4.6	-0.2
RN01	2021-07-08 06:50:04	4.8	-0.4
RN01	2021-07-08 13:27:45	5.0	-0.6
RN01	2021-07-08 14:00:14	5.0	-0.4
RN01	2021-07-12 19:56:24	4.7	-0.6
RN01	2021-07-12 22:40:00	4.7	0.0
RN01	2021-07-13 06:13:08	5.2	-0.6
RN01	2021-07-13 07:13:43	4.0	-0.6
RN01	2021-07-22 11:14:50	4.6	-0.6
RN01	2021-07-22 11:37:20	4.6	-0.6
RN01	2021-07-22 14:04:26	4.4	-0.9
RN01	2021-07-23 00:33:47	4.8	0.0
RN01	2021-08-03 06:15:55	3.4	-0.6
RN01	2021-08-20 03:06:53	3.4	-0.4
RN01	2021-08-22 22:58:37	4.6	-0.6
RN01	2021-09-03 00:04:34	1.7	-0.9
RN01	2021-09-07 22:23:55	4.6	-0.4
RN01	2021-09-09 17:45:29	5.1	-0.4
RN01	2021-09-10 23:44:28	1.6	-0.9
RN01	2021-09-11 07:13:12	6.3	0.0
RN01	2021-09-11 09:02:08	5.2	-0.6
RN01	2021-09-11 09:17:43	5.2	-0.6
RN01	2021-09-22 02:48:39	4.6	-0.4
RN01	2021-09-25 09:32:42	4.8	0.1
RN01	2021-09-25 15:51:10	1.6	-0.6
RN01	2021-09-28 13:50:04	4.7	0.3
RN01	2021-10-10 13:23:41	5.2	-0.6
RN01	2021-10-11 20:24:30	2.8	-0.6
RN01	2021-11-14 19:42:30	1.3	-1.5

Appendix C. Continued

Station	Origin Time (UTC)	Distance (mi)	Magnitude
RN01	2022-01-13 07:16:23	2.2	-0.9
RN01	2022-01-16 15:27:52	3.1	-0.6
RN01	2022-01-18 10:27:07	4.9	-0.9
RN01	2022-01-29 13:47:15	4.9	-0.9
RN01	2022-02-17 05:49:02	3.5	-0.2
RN01	2022-02-20 12:34:54	11.4	0.2
RN01	2022-02-24 17:39:47	2.9	-0.9
RN01	2022-04-05 01:49:37	2.8	-0.6
RN01	2022-04-29 06:25:55	2.5	0.0
RN01	2022-05-01 15:24:16	1.7	-0.9
RN01	2022-05-05 04:30:50	4.8	-0.2
RN01	2022-05-06 20:39:45	4.5	0.0
RN01	2022-05-25 06:47:22	5.2	0.6
RN03	2021-07-05 10:05:59	4.9	-0.2
RN03	2021-08-28 04:26:05	2.6	-0.6
RN03	2021-09-09 03:06:23	4.4	-0.2
RN03	2021-09-17 06:32:41	2.2	-0.9
RN03	2021-09-17 11:30:26	2.0	-1.5
RN03	2021-12-01 13:23:27	2.3	-0.9
RN03	2021-12-15 13:28:19	2.4	-0.2
RN03	2022-01-03 08:04:40	0.9	-1.5
RN03	2022-01-13 13:57:55	2.7	-0.9
RN03	2022-01-16 23:50:16	2.1	-0.9
RN03	2022-01-26 06:30:34	2.2	-0.2
RN03	2022-01-26 06:31:40	11.0	-0.4
RN03	2022-01-27 06:23:39	9.0	-0.6
RN03	2022-01-27 06:24:59	2.1	-1.5
RN03	2022-01-27 06:25:21	8.6	-0.4
RN03	2022-01-29 05:29:37	8.1	-0.6
RN03	2022-02-19 02:59:27	5.3	-0.6
RN03	2022-02-21 00:44:43	5.4	0.0
RN03	2022-03-24 15:40:09	9.3	0.4
RN03	2022-05-07 15:51:48	8.2	0.1
RN03	2022-05-08 16:19:55	8.6	0.7
RN03	2022-05-17 07:27:38	2.9	0.0

Station	Origin Time (UTC)	Distance (mi)	Magnitude
SG02	2021-07-26 04:25:25	10.8	0.4
SG02	2021-09-15 01:51:19	4.7	-0.2
SG02	2021-09-29 08:38:29	2.7	-0.6
SG02	2021-10-12 21:41:09	4.2	-0.2
SG02	2022-01-02 02:55:29	0.7	-0.9
SG02	2022-01-02 04:03:18	1.5	-0.9
SG02	2022-01-02 05:14:43	0.7	-0.9
SG02	2022-01-02 06:09:05	1.1	-1.5
SG02	2022-01-02 06:17:31	0.8	-1.5
SG02	2022-01-02 10:42:26	1.7	-1.5
SG02	2022-01-02 10:42:49	1.2	-0.9
SG02	2022-01-02 10:48:29	3.2	-0.2
SG02	2022-01-02 11:51:46	1.2	-0.9
SG02	2022-01-02 11:57:00	1.3	-0.6
SG02	2022-01-02 12:18:38	0.8	-1.5
SG02	2022-01-02 12:18:38	1.6	-0.9
SG02	2022-01-02 12:21:01	0.9	-0.9
SG02	2022-01-03 12:30:46	2.2	-1.5
SG02	2022-01-09 17:09:58	0.9	-1.5
SG02	2022-01-20 12:20:14	0.3	-1.5
SG02	2022-01-24 01:28:20	7.2	0.0
SG02	2022-02-03 16:55:07	1.7	-0.9
SG02	2022-02-04 15:32:10	0.8	-0.6
SG02	2022-02-19 23:46:09	0.7	-1.5
SG02	2022-02-20 17:52:44	0.4	-1.5
SG02	2022-02-23 12:25:55	0.6	-1.5
SG02	2022-05-01 16:32:47	0.7	-1.5
SG02	2022-05-17 07:28:46	3.8	-0.2
SG02	2022-05-17 09:57:40	5.8	0.3

End of table

[This page is intentionally blank.]

Appendix D: Literature Review

Prior Oil and Gas Production Can Limit the Occurrence of Injection-induced Seismicity: A Case Study in the Delaware Basin of Western Texas and South-eastern New Mexico, USA

Dvory and Zoback (2021), *Geology*
https://doi.org/10.1130/G49015.1

Key Points

- Areas of the Delaware Basin with a history of oil and gas production have reduced likelihood of injection-related induced seismicity.
- Reduced pore pressure from reservoir depletion moves the stress state for normal faults away from failure conditions.
- Triggered earthquakes primarily occur along NW-SE trending faults optimally oriented for slip.

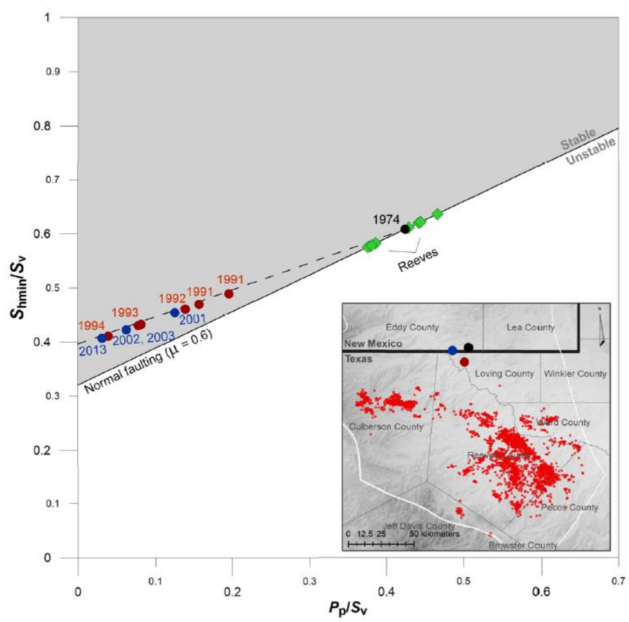

Figure D-1. Evolution of the state of stress in the Delaware Basin in terms of pore pressure (Pp) and least principal stress (Shmin), normalized by overburden stress (Sv). Dashed line represents the stress path in the case of reservoir depletion where the stress state moves toward a stable state where induced seismicity is less likely to occur. Map shows locations of wells corresponding to pore-pressure data points shown with the same color and smaller earthquake locations (small red dots). (From Dvory and Zoback, 2021).

Recent Water Disposal and Pore Pressure Evolution in the Delaware Mountain Group, Delaware Basin, Southeast New Mexico and West Texas, USA

Ge et al. (2021), *Journal of Hydrology: Regional Studies*
https://doi.org/10.1016/j.ejrh.2022.101041

Key Points

- A regional flow model was developed for the Delaware Mountain Group, a key injection zone for saltwater disposal in the Delaware Basin.
- Injection-related pressure increase is in the 0.7–2.8 MPa range, sufficient to create artesian conditions.
- Modelled pressure buildup is most sensitive to horizontal permeability and compressibility.

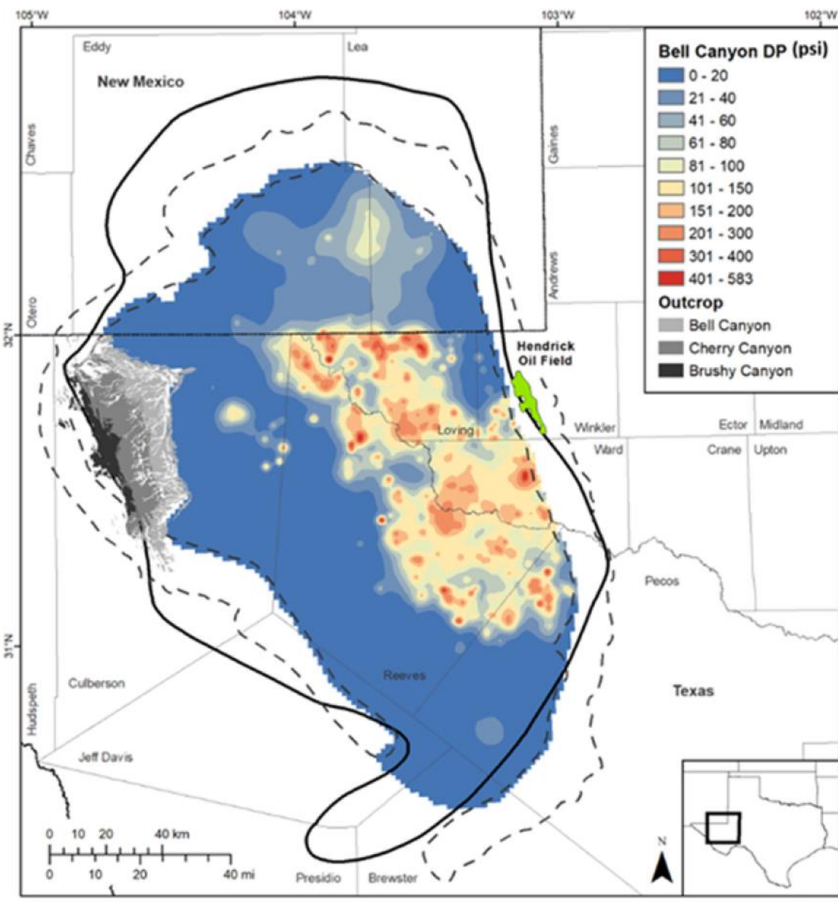

Figure D-2. Map of base case pressure increases in the Bell Canyon formation. (From Ge et al., 2021).

Wastewater Disposal Has Not Significantly Altered the Regional Stress State in Southern Kansas

Skoumal and Cochran (2021), *Seismological Research Letters*
https://doi.org/10.1785/0220210079

Key Points

- A previous study by Nolte et al. (2017) interpreted an apparent change in shear-wave anisotropy in south-central Kansas as a result of elevated pore pressure from high-volume saltwater disposal.
- New robust analysis indicates that the fast polarization direction did not vary with time and in-line with the direction of maximum horizontal stress, as expected.
- Apparent observations from the Nolte et al. (2017) study are likely a result of inconsistent source-receiver paths used in the analysis.

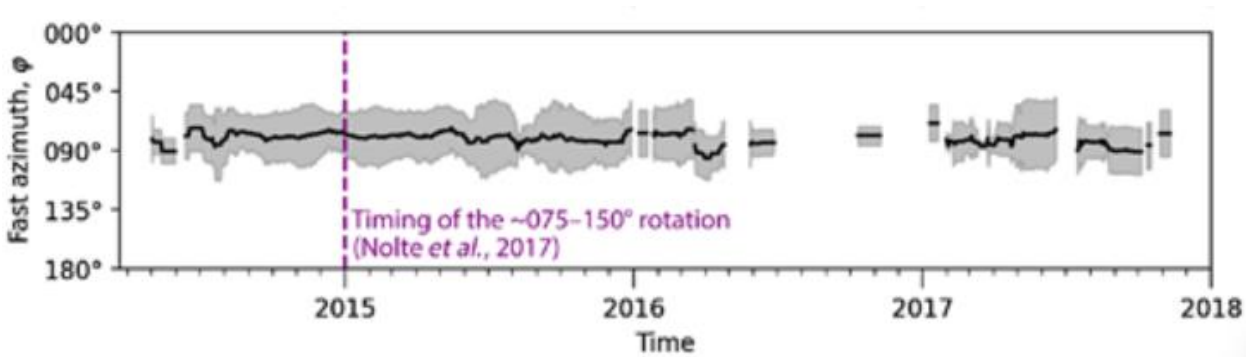

Figure D-3. Monthly average of φ (solid line) and 2σ (shaded region) for high-quality measurements. The timing of interpreted stress rotation (Nolte et al., 2017) from an east-northeast (~N75°E) to east-southeast (~S30°E) orientation is represented with a dashed line. (From Skoumal and Cochran, 2021).

Aftershock Triggering and Spatial Aftershock Zones in Fluid-Driven Settings: Discriminating Induced Seismicity from Natural Swarms

Karimi and Davidsen (2020), *Geophysical Research Letters*
https://doi.org/10.1029/2020GL092267

Key Points

- Significant event-event (aftershock) triggering is present in both natural fluid-driven swarms and injection-induced seismicity
- Both natural and induced fluid-driven settings are characterized by narrow aftershock zones
- Aftershock triggering is dominated by smaller triggers in induced seismicity but much less so for natural swarms

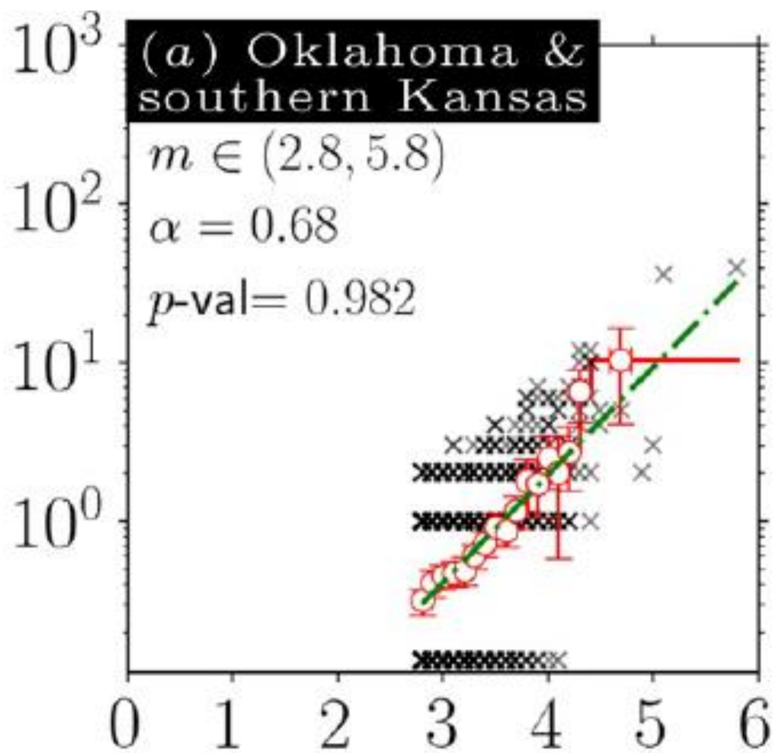

Figure D-4. Number of aftershocks N_{as} (m) as a function of trigger magnitude m in Oklahoma and southern Kansas. The symbols indicate the mean value N_{as} over prescribed bins. The error bars denote two times the standard error. The dash-dotted line indicates the productivity relation $N_{as} \propto 10^{\alpha m}$ fitted to the data over the specified magnitude range. The data points at the base of each panel indicate those events that did not trigger any aftershocks. (From Karimi and Davidsen, 2020).

Aeromagnetic Data Reveal Potential Seismogenic Basement Faults in the Induced Seismicity Setting of Oklahoma

Shah and Crain (2018), *Geophysical Research Letters*
https://doi.org/10.1029/2018GL077768

Key Points

- New aeromagnetic data suggest previously unmapped basement faults or contacts that are aligned with earthquake sequences in Oklahoma, suggesting earthquakes are occurring on reactivated ancient basement faults.
- Limited correlation with mapped faults suggests significant structural differences between the crystalline basement and sedimentary cover.
- Earthquake sequences terminating at aeromagnetic features suggest that intrusions locally inhibit induced seismicity due to fault termination or changes in permeability.

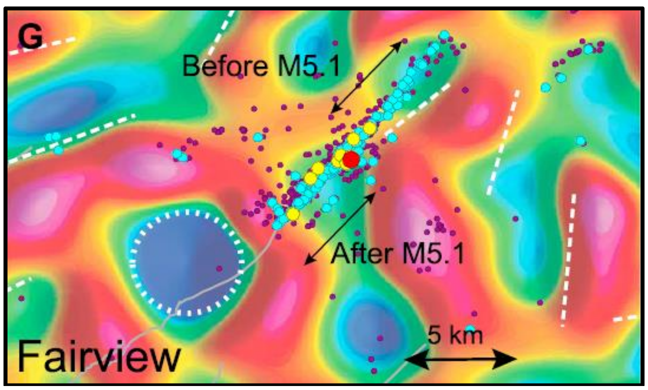

Figure D-5. Band-pass filtered anomaly near the Fairview sequence, which ruptured in two stages. The earlier rupture was aligned with a magnetic contact. White dotted circle delineates an interpreted intrusive body at the western end of the sequence. (From Shah and Crain, 2018).

[This page is intentionally blank.]